Smart Antenna Assignment is Essential in Full-Duplex Communications

José Mairton B. da Silva, Jr., *Member, IEEE*, Hadi Ghauch, *Member, IEEE*, Gábor Fodor, *Senior Member, IEEE*, Mikael Skoglund, *Fellow, IEEE*, and Carlo Fischione, *Senior Member, IEEE*

***Abstract*— Full-duplex communications have the potential to almost double the spectral efficiency. To realize such a potentiality, the signal separation at base station's antennas plays an essential role. This article addresses the fundamentals of such separation by proposing a new smart antenna architecture that allows every antenna to be either shared or separated between uplink and downlink transmissions. The benefits of such architecture are investigated by an assignment problem to optimally assign antennas, beamforming and power to maximize the weighted sum spectral efficiency. We propose a near-to-optimal solution using block coordinate descent that divides the problem into assignment problems, which are NP-hard, a beamforming and power allocation problems. The optimal solutions for the beamforming and power allocation are established while near-to-optimal solutions to the assignment problems are derived by semidefinite relaxation. Numerical results indicate that the proposed solution is close to the optimum, and it maintains a similar performance for high and low residual self-interference powers. With respect to the usually assumed antenna separation technique and half-duplex transmission, the sum spectral efficiency gains increase with the number of antennas. We conclude that our proposed smart antenna assignment for signal separation is essential to realize the benefits of multiple antenna full-duplex communications.**

***Index Terms*— Full-duplex systems, antenna assignment, beamforming design, power allocation, hardware impairments.**

I. Introduction

IN-BAND full-duplex (FD) communication overcomes the assumption that it is not possible for radios to transmit and receive simultaneously on the same time-frequency resource, and can almost double the spectral efficiency of conventional half-duplex (HD) wireless transmissions [1]–[3]. Until recently, in-band FD was not considered as a solution for wireless networks due to the inherent interference created from the transmitter to its own receiver, the so called self-interference (SI). However, recent advancements in antenna and analog/digital interference cancellation techniques demonstrate FD transmissions as a viable alternative to traditional HD transmissions [4]–[7].

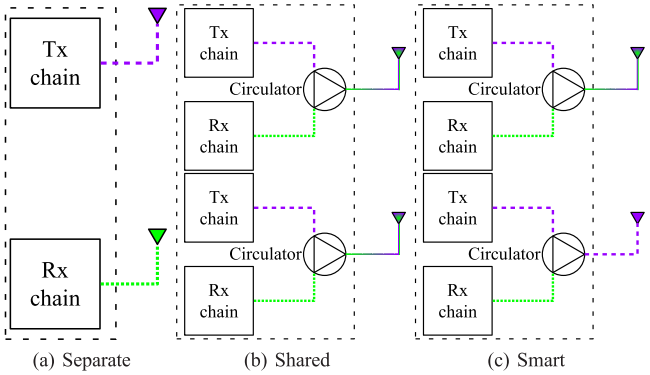

Fig. 1. An example of separate (or split), shared, and our proposed smart full-duplex architecture. We use purple dashed lines for Tx signal, green dotted lines for Rx signal, and a joint purple and green solid lines for simultaneous Tx and Rx signals.

To achieve simultaneous transmission and reception in FD, there are two architectures for separating the signals that split and share the available antennas respectively; see Figure 1 [1]. The first method consists of physically separating (or splitting) the transmitter/receiver chains and antennas, i.e., using a subset of antennas to transmit and the other part to receive (see Figure 1a). The second method shares all the antennas in the transmitter/receiver chains, and uses an analog device, such as a circulator, to separate the receiver from the transmitter (see Figure 1b). Note the different colours and line types for transmitter (purple dashed), receiver (green dotted), and simultaneous transmission and reception signals (purple and green solid). For simplicity, we refer to these two architectures as shared and separated (or split). Irrespectively of the antenna architecture, the presence of the residual SI requires further interference mitigation using a combination of analog and/or digital cancellation [2]. The architecture impacts the number of available antennas for transmission and reception, as well as the characteristics of the self-interference channel, and the power at which the uplink (UL) and downlink (DL) signals are received. Consequently, it is crucial to understand which architecture should be used for the UL/DL antennas of multi-antenna FD cellular networks.

Manuscript received August 31, 2020; revised December 11, 2020; accepted January 26, 2021. Date of publication February 15, 2021; date of current version May 18, 2021. The work of J. M. B. da Silva Jr. was supported by the Brazilian National Council for Scientific and Technological Development (CNPq). He would like to acknowledge the Lars Hierta Memorial Foundation for partially supporting this work. G. Fodor was partially sponsored by the Ericsson-KTH project SPECS II. The associate editor coordinating the review of this article and approving it for publication was L. Song. *(Corresponding author: José Mairton B. da Silva.)*

José Mairton B. da Silva, Jr., Mikael Skoglund, and Carlo Fischione are with the School of Electrical Engineering and Computer Science, KTH Royal Institute of Technology, 114 28 Stockholm, Sweden (e-mail: jmbdsj@kth.se).

Hadi Ghauch is with the COMELEC Department, Telecom-Paris, IMT, 75634 PARIS CEDEX 13, France.

Gábor Fodor is with the School of Electrical Engineering and Computer Science, KTH Royal Institute of Technology, 114 28 Stockholm, Sweden, and also with Ericsson Research, 164 40 Kista, Sweden.

Color versions of one or more figures in this article are available at https://doi.org/10.1109/TCOMM.2021.3059463.

Digital Object Identifier 10.1109/TCOMM.2021.3059463

This work is licensed under a Creative Commons Attribution 4.0 License. For more information, see https://creativecommons.org/licenses/by/4.0/

In this article, we focus on understanding the impact of the two antenna architectures for full-duplex communications on key performance metrics such as the achieved spectral efficiency. To this end, we propose a third architecture that we call smart architecture (see Figure 1c), which is an intermediate between the two aforementioned architectures and a generalization of the shared architecture. Our proposed smart architecture allows the base station (BS) to decide between sharing a specific antenna to achieve simultaneous transmissions in the UL and DL, or to dedicate it to either UL or DL transmission at a time. For example, Figure 1c shows one antenna with simultaneous transmissions in the UL and DL and another antenna with only DL transmission. With this, the design freedom to allocate the antennas increases but the design challenge increases as well. Apart from the inherently present SI from the DL (transmitting) to the UL (receiving) antennas, our smart architecture must also deal with user equipment (UE)-to-UE and multiple input multiple output (MIMO) multi-user interference. This smart architecture allows us to evaluate whether it is more advantageous to share all antennas or to select a subset to be separated between UL and DL. In practice, it may be complicated to share between UL and DL a large number of antennas due to the large number of analog devices necessary for the SI cancellation. Accordingly, our proposed smart architecture explores the technology potential of the smart antenna assignment for a FD system. Specifically, we aim to show the potential of the smart antenna architecture. To achieve this, we select as performance metric the maximization of the weighted sum spectral efficiency. We assume a single-cell system with multiple users and antennas at the BS while considering antenna assignment, transmitter and receiver distortions [8], beamforming, and power allocation. We show that this problem is a mixed integer nonlinear programming problem, which is known for its high complexity and computational intractability [9] and whose continuous variables are the DL beamforming and UL power allocation.

Due to the high complexity of the optimization problem, we build on the equivalence between sum rate maximization and weighted minimum mean square error (WMMSE) minimization [10]. We thus rewrite the problem as a WMMSE minimization and use the block coordinate descent (BCD) optimization method to solve the problem iteratively [11]. We partition the problem into blocks of variables, and the solution for each block is obtained assuming that all variables in other blocks remain fixed. We obtain the optimal beamforming in the DL and the optimal power allocation in the UL in closed form. Nevertheless, the UL and DL antenna assignment variables are binary (as well as NP-hard), which make the use of BCD in our problem nontrivial. Indeed, having globally optimal solutions for each blocks is a necessary condition for showing the convergence of BCD. To obtain an approximate solution with provable optimality gap for these blocks, we rewrite the problem as a semidefinite programming (SDP) problem and resort to semidefinite relaxation (SDR) with randomization [12]. We prove that convergence to stationary point of the sum-rate maximization problem is achieved when the solution given by SDR is optimal. Although BCD and SDR are known methods in the optimization literature, our contribution is the combination of both optimization methods to provide a nontrivial solution for mixed-integer nonlinear problems.

The numerical results demonstrate that the optimality gap between an exhaustive solution of the WMMSE minimization problem and the proposed solution is small. We benchmark the proposed solution against HD transmissions and a simple split antenna architecture, in which the antennas are split equally between UL and DL. The proposed solution provides high gains with respect to HD, ranging from 46% to 91%, as well as to the split antenna solution. We notice that by allowing a smart sharing and splitting of UL and DL antennas, our solution is robust against the effects of the residual SI. We also analyse scenarios with traffic asymmetry between UL and DL, in which the results show that the split antenna solution is a good candidate when the residual SI is high. Furthermore, we also consider a scenario when the number of antennas at the BS and users in the cell grows proportionally, in which the results show that the performance gains with respect to HD transmissions and the split architecture grow with the number of antennas. Our overall finding is that smart antenna assignment, including sharing/splitting of antennas between UL and DL, is essential because it is advantageous in many scenarios and is resilient against effects of the residual SI power.

The remainder of the article is organized as follows. Section II discusses relevant and closely related works. Section III presents the system model and main parameters, followed by the problem formulation. Section IV analyses the solution approach for the WMMSE minimization problem. Using block coordination descent, we arrive at a sequence of block variables that are solved iteratively. For the beamforming and power allocation, the optimal solutions in closed form are provided, while for the antenna assignment variables the solutions provided are close-to-optimal. Section V provides the convergence, complexity analysis, and the also the detailed channel information acquisition necessary for the proposed solution to run. Section VI presents numerical results and compares the performance of the proposed solution with the split antenna architecture and HD transmissions for many scenarios, including different residual SI powers and number of antennas.

II. Related Works

Shared and separate architecture in FD radios have origins in continuous wave radar systems [1]. In the wireless communication community, these architectures have been studied mainly from an experimental perspective.

The antenna techniques used to allow simultaneous transmission and reception are considered as passive suppression of the SI. Differently from the active suppression of the SI, passive suppression propose to be used before the SI enters the receiver chain circuit [1], [4]. In [1], the authors highlight that a FD radio with M transmit and receive chains requires $2N$ antennas in a separate architecture, whereas it requires M antennas, $2M$ transmit and receive chains, and M circulators in a shared antenna implementation. For a compact radio, the separate antenna architecture may be difficult to implement

properly due to the spacing between antennas, whereas the shared antenna architecture may be challenging to employ in a large antenna scenario due to the number of circulators. In [13], the authors mention that some degree of freedom is lost in the spatial domain using antenna splitting techniques. Since the decision on the type of passive suppression is primarily based on hardware experiments, the experimental works have been among the first to consider either separating [4], [14]–[16] or sharing the antennas [5], [7], [17], [18].

Most of the works in FD networks have assumed that the antenna architecture has already been decided, which have led the works to analyse the theoretical improvement achieved by FD [8], [19]–[21]. The authors in [8] have analysed the achievable rates of FD MIMO relaying, while assuming practical transmitter/receiver distortions. In [19], the authors have devised beamforming and power control mechanisms to maximize the spectral efficiency in FD multiple input single output (MISO) cellular networks. The work in [22] has proposed a user selection algorithm to maximize the spectral efficiency in FD MISO cellular networks, while fixed power and beamforming in the UL and DL are assumed. The authors in [20] have proposed a beamforming design for spectral efficiency maximization in FD multi-cell MIMO cellular networks, in which FD users as well as transmitter/receiver distortions are taken into account. The works just mentioned above have assumed that the antennas are split between UL and DL, while the authors in [21] have assumed the shared antenna architecture. Using the duality between UL and DL channels, the authors in [21] have aimed to maximize the sum rate in a single cell cellular network.

Nevertheless, some works in the literature have addressed the general topic of antenna splitting [23]–[26]. The authors in [23] have considered antenna selection in a bidirectional FD system with two antennas to maximize the sum rate or minimize the symbol error rate, while operating in a point-to-point single-antenna scenario. The authors in [24] have analysed SI cancellation via digital beamforming for large-antennas FD communications. Their proposed solution highlights the importance of UL/DL antenna splitting and assumes a fixed splitting. Similarly, the work in [25] has devised antenna splitting and beamforming to minimize the gap between demand and achievable rates. Assuming a given number of full-duplex antennas with analog cancellation, and ignoring the UE-to-UE interference between single-antenna UL and DL users, the proposed suboptimal algorithm splits the antennas and evaluates the DL beamforming to minimize the self-interference on receive antennas. In contrast, the work in [26] has considered that the antennas must be split, but the precise splitting between UL and DL is unknown. The authors proposed an antenna assignment algorithm to minimize the sum mean squared error (MSE) while considering transmit and receiver distortions.

However, these works differ from ours in that they do not consider that every antenna has the possibility of sharing or splitting. With the possibility of antenna assignment between sharing or splitting, we can understand the fundamental trade-offs between both separate and shared antenna architectures, and further increase the spectral efficiency of full-duplex systems. In addition to the antenna assignment, we take into account the transmit and receiver distortions, beamforming and power allocation in the sum rate maximization problem. In the light of this survey of related literature, the main contributions of this article are as follows:

- We propose a new smart antenna assignment between UL and/or DL antennas while considering transmitter and receiver distortions, beamforming and power allocation. We show the fundamental performance limits of the proposed by an optimization problem where we maximize the weighted sum spectral efficiency in FD cellular networks, which is a natural performance metric in cellular systems.
- Due to the complexity of the optimization, which is mixed integer nonlinear and has no known solution method, we use the equivalence between sum rate maximization and WMMSE minimization. Using BCD, we separate the problem in blocks of variables for which we derive the optimal analytical solutions of the beamforming and power allocation problems. For the assignment blocks, in which the resulting optimization problems are NP-hard, we resort to SDR with randomization to obtain solutions with provable optimality gap. Using Propositions 1-4 and Theorem 2, we show that convergence is achieved by combining BCD and SDR which is new in the literature.
- We evaluate the proposed solution by a realistic system simulator and gain insights that help design the antenna architecture for FD cellular networks operating traffic asymmetry, different residual SI powers, and scenarios with many antennas and users. Specifically, we show that smart antenna sharing/splitting is advantageous and outperforms HD and fixed antenna architectures.

For notations, vectors and matrices are denoted by bold lower and upper case letters, respectively; $\mathbf{A}^{\mathrm{H}}$ is the Hermitian of $\mathbf{A}$; $\mathrm{Diag}\,(\mathbf{A})$ is the column vector created from the diagonal of matrix $\mathbf{A}$; similarly, $\mathrm{diag}(\mathbf{A})$ or $\mathrm{diag}(\mathbf{a})$ are the diagonal matrices whose elements are in the diagonal of matrix $\mathbf{A}$, or composed by vector $\mathbf{a}$ in the diagonal, respectively. We denote by $\mathbf{I}_K$ the identity matrix of dimension K, by $\mathbf{0}$ and $\mathbf{1}$ a vector or matrix where all elements are zero or one, respectively, and by $\mathbb{C}$ the complex field. We denote expectation by $\mathbb{E}\{\cdot\}$, the circular complex Gaussian distribution with mean vector $\boldsymbol{\mu}$ and covariance matrix $\boldsymbol{\Sigma}$ by $\mathcal{CN}(\boldsymbol{\mu}, \boldsymbol{\Sigma})$. We define a stationary point [11], or critical point, $\bar{\mathbf{x}} \in \mathcal{X}$ as the point that satisfies $\nabla f(\bar{\mathbf{x}})^{\mathrm{T}}(\mathbf{y} - \bar{\mathbf{x}}) \geq 0$, for every $\mathbf{y} \in \mathcal{X}$, where $\nabla f(\mathbf{x}) \in \mathbb{R}^n$ denotes the gradient of f at $\mathbf{x}$.

III. System Model and Problem Formulation

A. System Model

We consider a single-cell cellular system in which the BS is FD capable, while the UEs served by the BS are HD capable, as illustrated by Figure 2. The BS is equipped with M antennas, which can be used to serve simultaneously I UL and J DL single-antenna users. In the figure, the BS is subject to SI from all of the antennas, whereas the UEs

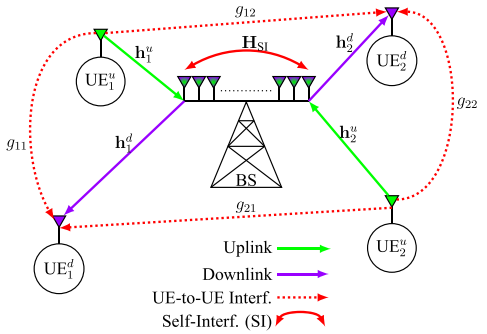

Fig. 2. An example of a multi-antenna cellular network employing FD with two UE pairs. The BS may use simultaneously on UL and DL all of its antennas, represented by the color gradient, which causes SI to all the antennas. To mitigate all interferences, it is advantageous to analyse the sharing/splitting of antennas between UL and DL, as well as devise transceivers for UL/DL users.

in the UL (UE_1^u and UE_2^u) cause UE-to-UE interference to co-scheduled UEs in the DL (UE_1^d and UE_2^d). We consider a multi-user MIMO scenario, i.e., a scenario in which all users share the time-frequency resources and are separated in the spatial domain. This scenario has been commonly adopted by the full-duplex community [19]–[21].

We let s_i^u and s_j^d denote the transmitted data symbol in the UL and DL, respectively, where both are zero mean with unit power. The transmitted power in the UL is denoted by $q_i^u \in \mathbb{R}$. In the DL, the data symbol s_j^d is multiplied by the beamforming vector $\mathbf{w}_j^d \in \mathbb{C}^{M\times 1}$ before transmission. Let $\mathbf{h}_i^u \in \mathbb{C}^{M\times 1}$ denote the complex channel vector comprising slow fading, shadowing, and path-loss between transmitter UE i and the BS, $\mathbf{h}_j^d \in \mathbb{C}^{M\times 1}$ denote the channel vector between the BS and receiving UE j, and $g_{ij} \in \mathbb{C}$ denote the interfering channel gain between the UL transmitter UE i and the DL receiver UE j.

Let $\mathbf{H}_{\text{SI}} \in \mathbb{C}^{M\times M}$ denote the SI channel matrix from the transmit antennas in DL to the receive antennas in the UL, which is modelled as Rician fading as suggested by experiments [4], [19]. Accordingly, $\mathbf{H}_{\text{SI}} \sim \mathcal{CN}\left(\sqrt{\sigma_{\text{SI}}^2 K/(1+K)}\mathbf{1}_{M\times M}, \left(\sigma_{\text{SI}}^2/(1+K)\right)\mathbf{I}_M\right)$, where $K = 0$ dB and 30dB are appropriate values for the Rician factors after the cancellation [4]. In this model, σ_{SI}^2 represents the ratio between the average SI power before and after the cancellation. We assume the far-field condition for the SI channel, which is common for frequencies below 6GHz in the literature [8], [19]–[21]. We set the central frequency of our system to 2.5GHz, which has a wavelength of 12cm and provides a Fraunhofer distance of 12cm. In a rectangular array with multiple antennas, the transmit and receive antennas can be further separated using different partitions such as east-west, north-south [24]. For instance, distances of 30cm or more are reported in the experimental results of [15]. The channel state information (CSI) is assumed known at the BS, which is also in accordance with some works in the full-duplex literature [19], [27]. Nevertheless, we detail how to acquire the necessary CSI to perform our proposed algorithm in Section V-C.

The signal received by the BS in the UL, and by DL user j, respectively, can be written as

$$\mathbf{y}^u = \sum_{i=1}^{I} \mathbf{h}_i^u\left(\sqrt{q_i^u}s_i^u + c_i^u\right) + \mathbf{H}_{\text{SI}}\left(\sum_{j=1}^{J}\mathbf{w}_j^d s_j^d + \mathbf{c}^d\right) + \boldsymbol{\eta}^u + \mathbf{e}^u, \tag{1a}$$

$$y_j^d = \mathbf{h}_j^{d\text{H}}\left(\sum_{m=1}^{J}\mathbf{w}_m^d s_m^d + \mathbf{c}^d\right) + \sum_{i=1}^{I} g_{ij}\left(\sqrt{q_i^u}s_i^u + c_i^u\right) + \eta_j^d + e_j^d, \tag{1b}$$

where $\boldsymbol{\eta}^u \sim \mathcal{CN}\left(\mathbf{0}_M, \sigma^2\mathbf{I}_M\right)$ and $\eta_j^d \sim \mathcal{CN}\left(0, \sigma^2\right)$ are additive white Gaussian noise at the BS and at DL user j, respectively. Notice that the second term in Eq. (1a) denotes the SI, whereas the second term in Eq. (1b) denotes the UE-to-UE interference from UL to DL users. In addition to both interferences terms, the multi-user interference is also present, which is represented in the first summation of Eqs.(1a)-(1b).

To account for non-ideal circuitry in the limited dynamic range, commonly referred to as hardware impairments, we consider an additional additive white Gaussian distortion signal at the transmitter and receiver [8]. These signals are modelled in the UL as $c_j^u \in \mathbb{C}$ and $\mathbf{e}^u \in \mathbb{C}^{M\times 1}$, and in the DL as $\mathbf{c}^d \in \mathbb{C}^{M\times 1}$ and $e_j^d \in \mathbb{C}$, respectively. The transmitter distortion has variance κ times the energy of the intended transmit signal at that antenna. Moreover, the receiver distortion has variance β times the energy collected by that antenna. Following previous works [8], [27], we define the transmitter distortions in the UL as $c_i^u \sim \mathcal{CN}\left(0, \kappa q_i^u\right)$, and in the DL as $\mathbf{c}^d \sim \mathcal{CN}\left(\mathbf{0}_M, \kappa\sum_{j=1}^{J}\text{diag}(\mathbf{w}_j^d\mathbf{w}_j^{d\text{H}})\right)$, where typically $\kappa \ll 1$. Similarly, we write the receiver distortion in the UL as $\mathbf{e}^u \sim \mathcal{CN}\left(\mathbf{0}_M, \beta\,\text{diag}(\boldsymbol{\Phi}^u)\right)$, and in the DL as $e_j^d \sim \mathcal{CN}\left(0, \beta\Phi^d\right)$, where typically $\beta \ll 1$. Furthermore, $\boldsymbol{\Phi}^u$ and Φ^d are the covariance matrix and variance of the receiver undistorted vector in the UL and at DL user j, respectively. We write $\boldsymbol{\Phi}^u$ and Φ^d as

$$\boldsymbol{\Phi}^u = \sum_{l=1}^{I} q_l^u\mathbf{h}_l^u\mathbf{h}_l^{u\text{H}} + \sum_{j=1}^{J}\mathbf{H}_{\text{SI}}\mathbf{w}_j^d\mathbf{w}_j^{d\text{H}}\mathbf{H}_{\text{SI}}{}^{\text{H}}, \tag{2a}$$

$$\Phi^d = \sum_{i=1}^{I}|g_{ij}|^2 q_i^u + \sum_{m=1}^{J}\mathbf{h}_m^{d\ \text{H}}\mathbf{w}_m^d\mathbf{w}_m^{d\ \text{H}}\mathbf{h}_m^d. \tag{2b}$$

With the modelling above, we closely approximate the combined effects of power amplifier noise, non-linearities in the analog-to-digital and digital-to-analog converters, as well as oscillator phase noise in practical hardware [8].

As illustrated in Figure 2, the M antennas at the BS may transmit and receive simultaneously, which can be done by the usage of circulators at each antenna element. For ease of notation, an antenna operating in a single direction, that is either transmitting in DL or receiving in UL, is in the *split or separate mode*. In contrast, an antenna operating in both directions simultaneously is in *full-duplex or shared mode*. Conversely, the smart antenna architecture can be seen as an intermediate mode between both separate or shared modes. It is complicated to realize the use of M antennas and circulators in practice, but one of our goals is to understand the trade-offs between the separate and shared architectures

by proposing a third architecture that balances between these two extremes. In terms of the number of Tx/Rx chains and also in terms of hardware requirements, the smart architecture is similar to the shared architecture (Figure 1b) as used in [5], [7], [17], [18]. Therefore, from a hardware requirement point of view, the requirement imposed on the smart antenna architecture is similar to those in the shared antenna architecture.

In order to analyse in which mode the antenna should operate, we define two binary assignment vectors, $\mathbf{x}^u, \mathbf{x}^d \in \{0,1\}^{M\times 1}$, for UL and DL, respectively, such that

$$x_{i(j)}^{u(d)} = \begin{cases} 1, & \text{if antenna } i \text{ } (j) \text{ is used on UL (DL)}, \\ 0, & \text{otherwise.} \end{cases} \tag{3}$$

However, it is useful to transform the assignment vectors into diagonal assignment matrices, such that $\mathbf{X}^u = \text{diag}\left(\mathbf{x}^u\right)$ and $\mathbf{X}^d = \text{diag}\left(\mathbf{x}^d\right)$. Notice that the antenna architecture affects both the hardware implementation and the signal model due to the difference in the number of antennas used. With the binary matrices, we are able to mathematically model the smart architecture as a combination between shared and separate antenna architectures. Using $\mathbf{X}^u$ and $\mathbf{X}^d$, the BS decides whether an antenna i will suffer SI from an antenna j or not. This is the case in situations where the SI signal is too strong, in which the antenna j in the DL might not be used, or in situations where the UE-to-UE interference signal is too strong, in which the antenna i antenna might not be used. To reflect the selected architecture on the signal model, we can apply $\mathbf{X}^u$ to the received UL symbol $\mathbf{y}^u$, creating the effective received symbol $\widetilde{\mathbf{y}}^u = \mathbf{X}^u\mathbf{y}^u$. Similarly, we can apply $\mathbf{X}^d$ to the transmitted signal $\sum_{m=1}^{J}\mathbf{w}_m^d s_m^d + \mathbf{c}^d$, creating the effective transmitted signal $\mathbf{X}^d\left(\sum_{m=1}^{J}\mathbf{w}_m^d s_m^d + \mathbf{c}^d\right)$.

With the antenna assignment, we can rewrite the signal models of Eqs. (1a)-(1b) as

$$\widetilde{\mathbf{y}}^u = \sum_{i=1}^{I}\widetilde{\mathbf{h}}_i^u(\sqrt{q_i^u}s_i^u + c_i^u) + \widetilde{\mathbf{H}}_{\text{SI}}\left(\sum_{j=1}^{J}\mathbf{w}_j^d s_j^d + \mathbf{c}^d\right) + \widetilde{\boldsymbol{\eta}}^u + \widetilde{\mathbf{e}}^u, \tag{4a}$$

$$\widetilde{y}_j^d = \widetilde{\mathbf{h}_i^u}^{\text{H}}\left(\sum_{m=1}^{J}\mathbf{w}_m^d s_m^d + \mathbf{c}^d\right) + \sum_{i=1}^{I} g_{ij}\left(\sqrt{q_i^u}s_i^u + c_i^u\right) + \eta_j^d + e_j^d, \tag{4b}$$

where $\widetilde{\mathbf{h}}_i^u = \mathbf{X}^u\mathbf{h}_i^u$, $\widetilde{\mathbf{h}}_j^d = \mathbf{X}^d\mathbf{h}_j^d$, $\widetilde{\mathbf{H}}_{\text{SI}} = \mathbf{X}^u\mathbf{H}_{\text{SI}}\mathbf{X}^d$ denote the effective UL, DL, and SI channels, respectively; $\widetilde{\boldsymbol{\eta}}^u = \mathbf{X}^u\boldsymbol{\eta}^u$ and $\widetilde{\mathbf{e}}^u = \mathbf{X}^u\mathbf{e}^u$ denote the effective noise and receiver distortion, with distributions $\widetilde{\boldsymbol{\eta}}^u \sim \mathcal{CN}\left(\mathbf{0}_M, \sigma^2\mathbf{X}^u\right)$, and $\widetilde{\mathbf{e}}^u \sim \mathcal{CN}\left(\mathbf{0}_M, \beta\mathbf{X}^u\,\text{diag}(\boldsymbol{\Phi}^u)\mathbf{X}^u\right)$, respectively.

We assume that the received signal, $\widetilde{\mathbf{y}}^u$, is linearly decoded at the BS by a filter $\mathbf{r}_i^u \in \mathbb{C}^{M\times 1}$. Similarly, the received signal of DL user j, $\widetilde{y}_j^d$, is linearly decoded by a filter $r_j^d \in \mathbb{C}$. Treating SI as noise, the signal-to-interference-plus-noise ratio (SINR) at the BS of transmitting user i and the SINR at the receiving user j of the BS are given by

$$\gamma_i^u = \frac{q_i^u\left|\mathbf{r}_i^{u\text{H}}\widetilde{\mathbf{h}}_i^u\right|^2}{\mathbf{r}_i^{u\text{H}}\boldsymbol{\Psi}_i^u\mathbf{r}_i^u}, \quad \gamma_j^d = \frac{\left|r_j^{d\text{H}}\widetilde{\mathbf{h}_j^d}^{\text{H}}\mathbf{w}_j^d\right|^2}{\left|r_j^d\right|^2\Psi_j^d}, \tag{5}$$

where $\boldsymbol{\Psi}_i^u$ and Ψ_j^d are the covariance matrix and variance of the total interference plus noise in the UL and DL, respectively; see (6a)-(6b), as shown at the bottom of the page. Notice that the r_j^d term in the numerator and denominator can be nulled out, but the beamforming and interference terms in the numerator and denominator still depend on r_j^d. We leave both terms in the numerator and denominator to directly express such dependency.

Thus, the achievable sum spectral efficiency (in bps/Hz) for UL and DL users are given by

$$R_i^u = \log_2(1+\gamma_i^u), \quad R_j^d = \log_2(1+\gamma_j^d). \tag{7}$$

In addition to the spectral efficiency, we consider priorities for the UL and DL users, which are denoted by α_i^u and α_j^d, respectively. As a special case, our approach includes sum rate maximization with $\alpha_i^u = \alpha_j^d = 1$, for path loss compensation with $\alpha_i^u = \left|\widetilde{\mathbf{h}_i^u}\right|^{-2}$ and $\alpha_j^d = \left|\widetilde{\mathbf{h}_j^d}\right|^{-2}$, and for traffic requirements as $\sum_i \alpha_i^u = 0.2$ and $\sum_i \alpha_i^u = 0.8$ to represent traffic asymmetry of 20% and 80% of UL and DL transmissions, respectively.

B. Problem Formulation

Our goal is to explore the technology potential of the smart antenna architecture on the UL and DL antennas, and show how good the propose smart architecture is. To this end, we aim to maximize the weighted sum spectral efficiency of all users, while jointly considering the assignment of UL and DL antennas, as well as the transmit and receiver beamforming variables. Specifically, we formulate the joint antenna assignment and transceiver design problem

$$\underset{\substack{\mathbf{x}^u,\mathbf{x}^d,\{q_i^u\}\\ \{\mathbf{w}_j^d\},\{\mathbf{r}_i^u\},\{r_j^d\}}}{\text{maximize}} \quad \sum_{i=1}^{I}\alpha_i^u R_i^u + \sum_{j=1}^{J}\alpha_j^d R_j^d \tag{8a}$$

$$\boldsymbol{\Psi}_i^u = \sum_{l\neq i}^{I} q_l^u\widetilde{\mathbf{h}}_l^u\widetilde{\mathbf{h}_l^u}^{\text{H}} + \kappa\sum_{l=1}^{I} q_l^u\widetilde{\mathbf{h}}_l^u\widetilde{\mathbf{h}_l^u}^{\text{H}} + \sum_{j=1}^{J}\widetilde{\mathbf{H}}_{\text{SI}}\left(\mathbf{w}_j^d\mathbf{w}_j^{d\text{H}} + \kappa\,\text{diag}\left(\mathbf{w}_j^d\mathbf{w}_j^{d\text{H}}\right)\right)\widetilde{\mathbf{H}}_{\text{SI}}^{\text{H}} + \beta\sum_{l=1}^{I} q_l^u\,\text{diag}\left(\widetilde{\mathbf{h}}_l^u\widetilde{\mathbf{h}_l^u}^{\text{H}}\right) + \beta\sum_{j=1}^{J}\text{diag}\left(\widetilde{\mathbf{H}}_{\text{SI}}\mathbf{w}_j^d\mathbf{w}_j^{d\text{H}}\widetilde{\mathbf{H}}_{\text{SI}}^{\text{H}}\right) + \sigma^2\mathbf{X}^u, \tag{6a}$$

$$\Psi_j^d = \sum_{m\neq j}^{J}\widetilde{\mathbf{h}_m^d}^{\text{H}}\mathbf{w}_m^d\mathbf{w}_m^{d\text{H}}\widetilde{\mathbf{h}_m^d} + \kappa\sum_{m=1}^{J}\widetilde{\mathbf{h}_m^d}^{\text{H}}\text{diag}\left(\mathbf{w}_m^d\mathbf{w}_m^{d\text{H}}\right)\widetilde{\mathbf{h}_m^d} + \sum_{i=1}^{I}|g_{ij}|^2 q_i^u(\kappa+\beta+1) + \beta\sum_{m=1}^{J}\widetilde{\mathbf{h}_m^d}^{\text{H}}\mathbf{w}_m^d\mathbf{w}_m^{d\text{H}}\widetilde{\mathbf{h}_m^d} + \sigma^2. \tag{6b}$$

$$\text{subject to } q_i^u \le P_{\max}^u, \quad \forall i, \tag{8b}$$

$$\sum\nolimits_{j=1}^{J} \operatorname{tr}\left(\mathbf{w}_j^d \mathbf{w}_j^{d\mathrm{H}}\right) \le P_{\max}^d, \tag{8c}$$

$$\mathbf{x}^u, \mathbf{x}^d \in \{0,1\}^{M\times 1}. \tag{8d}$$

The optimization variables are $\mathbf{x}^u, \mathbf{x}^d$, $\{q_i^u\}, \{\mathbf{r}_i^u\}$ for all i, and $\{\mathbf{w}_j^d\}, \{r_j^d\}$ for all j. Constraints (8b)-(8c) limit the transmit power per-user and the total DL power, while constraint (8d) ensures that the assignment variables are binary. The optimization problem (8) is a mixed integer nonlinear programming problem, which is known for its high complexity and computational intractability [9].

In order to solve problem (8), we adopt the equivalence between weighted sum rate maximization and sum WMMSE minimization [10]. Then, let us first define the MSE of the received symbol by UL user i as

$$E_i^u = \mathbb{E}\left\{\left\|\mathbf{r}_i^{u\mathrm{H}}\widetilde{\mathbf{y}}^u - s_i^u\right\|_2^2\right\} = \left|\sqrt{q_i^u}\mathbf{r}_i^{u\mathrm{H}}\widetilde{\mathbf{h}}_i^u - 1\right|^2 + \mathbf{r}_i^{u\mathrm{H}}\mathbf{\Psi}_i^u\mathbf{r}_i^u. \tag{9}$$

Similarly, let us define the MSE of the received symbol of DL user j as

$$E_j^d = \mathbb{E}\left\{\left\|r_j^{d\mathrm{H}}\widetilde{y}_j^d - s_j^d\right\|_2^2\right\} = \left|r_j^{d\mathrm{H}}\widetilde{\mathbf{h}_j^d}^{\mathrm{H}}\mathbf{w}_j^d - 1\right|^2 + \left|r_j^d\right|^2\Psi_j^d. \tag{10}$$

Using the MSEs definitions, the equivalence between weighted sum rate maximization and sum WMMSE minimization is established in the following theorem.

Theorem 1: Let ρ_i^u and ρ_j^d denote the weight variables for UL user i and DL user j, respectively. The following problem is equivalent to problem (8):

$$\underset{\substack{\{\rho_i^u\},\{\rho_j^d\},\mathbf{x}^u,\mathbf{x}^d,\\ \{q_i^u\},\{\mathbf{w}_j^d\},\{\mathbf{r}_i^u\},\{r_j^d\}}}{\text{minimize}} \sum\nolimits_{i=1}^{I} \alpha_i^u\left(\rho_i^u E_i^u - \log(\rho_i^u)\right) + \sum\nolimits_{j=1}^{J} \alpha_j^d\left(\rho_j^d E_j^d - \log(\rho_j^d)\right) \tag{11a}$$

$$\text{subject to Constraints (8b)} - \text{(8d)}. \tag{11b}$$

Proof: See Appendix B. ∎

Problem (11) has an objective function that is more amenable to BCD optimization. Nonetheless, due to constraints on power allocation (8b)-(8c) and on full-duplex antennas (8d), the problem is still mixed integer nonlinear programming and highly nontrivial. Neither problem (8) nor problem (11) includes the time evolution of the UL and DL channels, and we leave this for future work. To approach a solution to problem (11), we use the general framework of BCD [11], which partitions the problem into blocks of variables, and optimizes each block at each iteration, while keeping the remaining variables fixed.

IV. Solution Approach Based on Block Coordinate Descent

To solve problem (11), we use the optimization framework of BCD [11], which provides optimality and convergence for alternating optimization problems under some general assumptions. BCD has the ability to partition the problem into blocks of variables, where each block is optimized at each iteration and provided that some general assumptions are met, the iterations are guaranteed to converge. With the antenna assignment variables, problem (11) is a mixed integer nonlinear programming problem, and BCD cannot be adopted along with integer variables due to the lack of guarantees in the block updates. To this end, we propose a new joint application of BCD and SDR, in which we prove that the updates are nondecreasing and converge to the stationary point of problem (11).

Specifically, we partition problem (11) into five general blocks of variables:

1) Weight block: $\{\rho_i^u, \rho_j^d\}$
2) Receiver block: $\{\mathbf{r}_i^u, r_j^d\}$;
3) Transmitter block: $\{\mathbf{w}_j^d, q_i^u\}$;
4) UL antenna block: $\{\mathbf{x}^u\}$;
5) DL antenna block: $\{\mathbf{x}^d\}$.

We derive solutions for the five distinct subproblems of (11). For the updates of the UL and DL weights ρ_i^u, ρ_j^d, we use equation (22) on Appendix B to obtain the optimal weights. In the following, we consider the receiver block in Section IV-A; the transmitter block in Section IV-B; and both UL and DL antenna blocks in Section IV-C.

A. Optimum Receiver Design

Under fixed beamforming vector and transmit power, $\mathbf{w}_j^d$ and q_i^u, and fixed assignment matrices $\mathbf{X}^u, \mathbf{X}^d$, problem (11) is unconstrained and jointly convex in the UL and DL receive filters, i.e., $\{\mathbf{r}_i^u, r_j^d\}$. Therefore, we can obtain the optimum MSE receiver by differentiating (11a) with respect to either $\mathbf{r}_i^u$ or r_j^d, and setting to zero. Notice that the derivatives are taken with respect to complex numbers, and we use herein the necessary definitions from [28, Chapter 4]. Thus, the optimum MSE receiver for UL and DL are

$$\mathbf{r}_i^u = \sqrt{q_i^u}\left(q_i^u\widetilde{\mathbf{h}_i^u}\widetilde{\mathbf{h}_i^u}^{\mathrm{H}} + \mathbf{\Psi}_i^u\right)^{-1}\widetilde{\mathbf{h}_i^u}, \tag{12a}$$

$$r_j^d = \widetilde{\mathbf{h}_j^d}^{\mathrm{H}}\mathbf{w}_j^d\left(\widetilde{\mathbf{h}_j^d}^{\mathrm{H}}\mathbf{w}_j^d\mathbf{w}_j^{d\mathrm{H}}\widetilde{\mathbf{h}_j^d} + \Psi_j^d\right)^{-1}, \tag{12b}$$

where in the UL special care must be taken, such that the inverse is taken disregarding the zero columns/rows due to the usage of $\mathbf{X}^u$ and $\mathbf{X}^d$. Notice that (12a)-(12b) correspond to the well-known minimum mean squared error (MMSE) receiver.

B. Optimum Transmitter Design

To obtain the DL beamforming vector $\mathbf{w}_j^d$ and the UL transmit power q_i^u, we now consider all the other variables fixed and known. With this, the objective function in (11a) is separable and can be written as a sum of $f^u(\{q_i^u\})$ and $f^d(\{\mathbf{w}_j^d\})$. Proposition 1 poses this formulation.

Proposition 1: Consider optimization problem (11). Then, its objective function in (11a) is separable and can be written as the sum of two quadratic functions: $f^u(\{q_i^u\})$ and $f^d(\{\mathbf{w}_j^d\})$.

Proof: See Appendix C. ∎

We consider the change of variable, $f^u(\{q_i^u\})$ as $\widetilde{q_i^u} = \sqrt{q_i^u}$, which is a one-to-one to mapping. Then, $f^u(\{\widetilde{q_i^u}\})$ is a convex quadratic function. With this, we can write problem (11) with $\{\widetilde{q_i^u}\}$ as the sole block of variables as

$$\underset{\{\widetilde{q_i^u}\}}{\text{minimize}} f^u(\{\widetilde{q_i^u}\}) \tag{13a}$$

$$\text{subject to } \widetilde{q_i^u}^2 \leq P_{\max}^u, \ \forall i, \tag{13b}$$

$$\widetilde{q_i^u} \geq 0, \ \forall i, \tag{13c}$$

Problem (13) is convex, and its optimal solution can be obtained using the Karush-Kuhn-Tucker (KKT) conditions. We express $\{\widetilde{q_i^u}\}$ as

$$\{\widetilde{q_i^u}\} = \left[\frac{\alpha_i^u \rho_i^u \operatorname{Re}\left\{ \mathbf{r}_i^{u\mathrm{H}} \widetilde{\mathbf{h}^u}_i \right\}}{\delta_i^u + \operatorname{tr}\left(\Delta_i^u \mathbf{R}^u\right) + \lambda_i} \right]^+, \tag{14}$$

where λ_i is the Lagrange multiplier related to constraints (13b), $[v]^+ = \max\{0, v\}$, and $\delta_i^u, \mathbf{\Delta}_i^u, \mathbf{R}^u$ are defined in (24). Note that the λ_i is found using the complementary slackness condition satisfying

$$\lambda_i(\widetilde{q_i^u}^2 - P_{\max}^u) = 0, \ \forall i. \tag{15}$$

The optimal transmitted power q_i^u is readily obtained as $q_i^u = \widetilde{q_i^u}^2$.

Similarly, we notice that $f^d(\{\mathbf{w}_j^d\})$ is a convex quadratic function of the beamforming vectors $\{\mathbf{w}_j^d\}$ because $\mathbf{\Sigma}_j^d$ in (25) is positive semidefinite. Therefore, we can rewrite problem (11) with $\{\mathbf{w}_j^d\}$ as the sole block of variables as

$$\underset{\{\mathbf{w}_j^d\}}{\text{minimize}} \ f^d(\{\mathbf{w}_j^d\}) \tag{16a}$$

$$\text{subject to } \sum\nolimits_{j=1}^{J} \operatorname{tr}\left(\mathbf{w}_j^d \mathbf{w}_j^{d\mathrm{H}}\right) \leq P_{\max}^d, \tag{16b}$$

Problem (16) is a convex quadratic problem in $\{\mathbf{w}_j^d\}$. Using the KKT conditions, we express $\mathbf{w}_j^d$ in closed-form solution as

$$\mathbf{w}_j^d = \alpha_j^d \rho_j^d r_j^{d\mathrm{H}} \left(\mathbf{\Sigma}_j^d + \mu \mathbf{I}_M\right)^{-1} \widetilde{\mathbf{h}_j^d}^{\mathrm{H}}, \tag{17}$$

where $\mathbf{\Sigma}_j^d$ is defined in (26), and the Lagrange multiplier μ is found using the complementary slackness condition satisfying

$$\mu \left(\sum\nolimits_{j=1}^{J} \operatorname{tr}\left(\mathbf{w}_j^d \mathbf{w}_j^{d\mathrm{H}}\right) - P_{\max}^d \right) = 0. \tag{18}$$

With this, we find the optimal solution for the transmitter block by solving problem (13) to obtain q_i^u, and using Eqs. (17)-(18) to obtain $\mathbf{w}_j^d$.

C. Antenna Mode Selection

We now consider all the other variables fixed and known, and analyse the sum MSE problem separately with the antenna assignment matrices $\mathbf{X}^u$ and $\mathbf{X}^d$ as variables.

We can write the sum WMMSE in Eq. (11a) as the sum of two quadratic and one biquadratic functions that depend on $\mathbf{X}^u$ and $\mathbf{X}^d$: $f^u(\mathbf{X}^u)$, $f^d(\mathbf{X}^d)$, and $f^{u,d}(\mathbf{X}^u, \mathbf{X}^d)$, where they depend on $\mathbf{X}^u$, $\mathbf{X}^d$, and jointly on $\mathbf{X}^u$, $\mathbf{X}^d$, respectively. Notice that the UL block depends only on $\mathbf{X}^u$, which allow us to consider $f^{u,d}(\mathbf{X}^u, \mathbf{X}^d)$ with fixed $\mathbf{X}^d$, whereas the same applies for the DL block. Thus, we can write the UL objective function as $\widetilde{f^u}(\mathbf{X}^u) = f^u(\mathbf{X}^u) + f^{u,d}(\mathbf{X}^u, \mathbf{X}^d)|_{\mathbf{X}^d \text{fix}}$, and similarly in the DL as $\widetilde{f^d}(\mathbf{X}^d) = f^d(\mathbf{X}^d) + f^{u,d}(\mathbf{X}^u, \mathbf{X}^d)|_{\mathbf{X}^u \text{fix}}$. Proposition 2 poses this formulation.

Proposition 2: Consider optimization problem (11). Then, its objective function in (11a) can be written as the sum of two quadratic functions $f^u(\mathbf{X}^u)$, $f^d(\mathbf{X}^d)$ and one biquadratic function $f^{u,d}(\mathbf{X}^u, \mathbf{X}^d)$. Furthermore, the objective function of UL and DL block can be simplified into the quadratic functions $\widetilde{f^u}(\mathbf{X}^u)$ and $\widetilde{f^d}(\mathbf{X}^d)$.

Proof: See Appendix D. ∎

Using BCD and Proposition 2, we can write problem (11) as two separate problems; one with variable $\mathbf{X}^u$ using fixed $\mathbf{X}^d$, and another with variable $\mathbf{X}^d$ using fixed $\mathbf{X}^u$. We notice that both UL and DL functions have the same mathematical structure, and for ease of notation, we write the general antenna assignment problem

$$\underset{\mathbf{x}}{\text{minimize}} \ \widetilde{f}(\mathbf{X}) \tag{19a}$$

$$\text{subject to } \mathbf{x} \in \{0,1\}^{M \times 1}, \tag{19b}$$

where variable $\mathbf{X}$ and objective function $\widetilde{f}(\mathbf{X})$ can represent either UL and DL. When solving problem (19) for UL, we do not consider $f^d(\mathbf{X}^d)$ in the objective, and vice-versa. However, the structure of problem (19) is still difficult to handle due to the binary constraint on $\mathbf{X}^u$ or $\mathbf{X}^d$.

Therefore, we equivalently rewrite problem (19) as the homogeneous boolean quadratic problem; see Proposition 3.

Proposition 3: Consider problem (19). Then, problem (19) is equivalent to the boolean quadratic problem below:

$$\underset{\mathbf{z}}{\text{minimize}} \ \mathbf{z}^{\mathrm{T}} \mathbf{\Upsilon} \mathbf{z} + d \tag{20a}$$

$$\text{subject to } z_n \in \{-1, 1\}, \quad \forall n = 1, \ldots, M+1, \tag{20b}$$

Proof: See Appendix E. ∎

Problem (20) is a boolean quadratic problem, which belongs to the class of NP-hard problems [12], [29]. Problem (20) has high complexity, as the authors in [29] proved that finding the global minimum with unique solution is NP-hard. Due to the high complexity of problem (20), we resort to SDR. Semidefinite relaxation is a powerful and efficient approximation technique to solve nonconvex quadratic problems [12]. SDR has also been applied to the problem of maximum likelihood detection in CDMA systems [30], [31].

In the following result, we rewrite problem (20) into SDR form.

Proposition 4: Consider optimization problem (43). This problem can be relaxed using SDR formulation as

$$\underset{\mathbf{Z}}{\text{minimize}} \ \operatorname{tr}\left(\mathbf{\Upsilon} \mathbf{Z}\right) + d \tag{21a}$$

$$\text{subject to } [\mathbf{Z}]_{nn} = 1, \ \forall n = 1, \ldots, M+1 \tag{21b}$$

$$\mathbf{Z} \succeq 0. \tag{21c}$$

Proof: See Appendix F. ∎

Problem (21) is convex and can be solved using well-known solvers. However, the matrix provided by such solvers may not

have rank-1, which implies that we need to retrieve a rank-1 solution from the solution matrix. By suitably rounding in an appropriate manner the optimal solution of problem (21), we are able to provide feasible solutions to problem (20) and approximation guarantees. For a similar problem formulation in maximum likelihood detection in CDMA [31], the approximation obtained by randomization is tight and asymptotically optimal in the high signal to noise ratio (SNR) regime [32]. However, in our case this approximation does not apply because the distribution of the matrices and vectors necessary for the asymptotic analysis present in [32] are not present herein. Nevertheless, our numerical results show that the solution of problem (21) provides a tight solution for the UL block, and a small approximation gap for the DL block.

Algorithm 1 details the randomization used to approximate the solution of problem (20). The basic idea is to generate a binary vector $\mathbf{z}$ using the solution matrix $\mathbf{Z}^\star$ of problem (21) and random vectors $\boldsymbol{\xi}\sim\mathcal{N}(0,\mathbf{Z}^\star)$, which can be accomplished using Cholesky factorization. We generate L random samples $\boldsymbol{\xi}_l$, and select the sample set that provides the minimum value of the objective function in problem (21) (see lines 2-5). If the set has cardinality one, then select the optimal sample, and construct the vector $\mathbf{z}^\star$ with size $M\times 1$ (see line 8). Otherwise, select the optimal sample $\mathbf{z}_{n^\star}$ that has more active antennas, i.e., the sample that has more $+1$ than -1 (see lines 10-11). Then, we are able to approximate $\mathbf{x}^\star$ and finish the randomization procedure (see line 13).

Algorithm 1 Gaussian Randomization Procedure for Problem (21)

1: **Input**: SDR solution $\mathbf{Z}^\star$ and number of randomizations L
2: **for** $l=1,\ldots,L$ **do**
3: Generate $\boldsymbol{\xi}_l\sim\mathcal{N}(0,\mathbf{Z}^\star)$
4: Construct feasible point $\mathbf{z}_l=\mathrm{sgn}(\boldsymbol{\xi}_l)$
5: **end for**
6: Determine $\mathcal{L}=\{\mathbf{z}_n|\mathbf{z}_n=\arg\min_{l=1,\ldots,L}\mathbf{z}_l{}^{\mathrm{T}}\boldsymbol{\Upsilon}\mathbf{z}_l\}$
7: **if** $\mathrm{card}\,(\mathcal{L})=1$ **then**
8: Select $\mathbf{z}^\star=[\mathbf{z}_n]_{1:M}$
9: **else**
10: Select $n^\star=\arg\max_{n=1,\ldots,\mathrm{card}(\mathcal{L})}\mathbf{z}_n{}^{\mathrm{T}}(\mathbf{1}+\mathbf{z}_n)/2$
11: Select $\mathbf{z}^\star=[\mathbf{z}_{n^\star}]_{1:M}$
12: **end if**
13: Approximate $\mathbf{x}^\star=(\mathbf{z}^\star+1)/2$
14: **Output**: $\mathbf{x}^\star$ as the approximate solution for problem (19)

D. Summary of the Algorithm

The solution of the WMMSE problem (11) is named A-SDP and can be summarized as follows in Algorithm 2. The algorithm initializes the beamforming vectors $\mathbf{w}_j^d$ and transmitting powers q_i^u such that constraints (8b)-(8c) are fulfilled at equality; assigns identity matrices to $\mathbf{X}^u,\mathbf{X}^d$; and sets ρ_i^u,ρ_j^d as ones. Subsequently, we denote by n the iteration counter, and by f_0 the objective function of problem (11), and initialize it both as zero. The algorithm updates all the blocks sequentially until the convergence criterion is met, i.e., until the difference between previous and current update of the objective function f_0 is lower than or equal to the predefined threshold ζ. Notice that for the assignment blocks in the UL and DL, we only update the blocks if it leads to a decrease in the objective function f_0.

In Section V we present an in-depth theoretical analysis of Algorithm 2, including its convergence, complexity and the necessary information at each node for its implementation.

Algorithm 2 A-SDP: Solution of WMMSE Problem (11)

1: Initialize $\mathbf{h}_i^u,\mathbf{h}_j^d,\mathbf{H}_{\mathrm{SI}},g_{ij},\mathbf{w}_j^d,q_i^u,\mathbf{x}^u,\mathbf{x}^d,\rho_i^u,\rho_j^d,\zeta$
2: Set $n=0$ and $f_0(n)=0$
3: **while** $|f_0(n)-f_0(n-1)|>\zeta$ **do**
4: $n\leftarrow n+1$
5: Update $\{\mathbf{r}_i^u(n),r_j^d(n)\}$ using equations (12a)-(12b)
6: Update $\{q_i^u(n)\}$ using equation (14)-(15) or solving problem (13)
7: Update $\{\mathbf{w}_j^d(n)\}$ using equation (17)-(18) or solving problem (16)
8: Evaluate the objective function f_0 up to this point
9: Evaluate $\mathbf{x}^{u^\star}$ by solving problem (21) and using Algorithm 1
10: Evaluate the objective function with $\mathbf{x}^{u^\star}$: $f_0|_{\mathbf{x}^{u^\star}}$
11: **if** $f_0(n)|_{\mathbf{x}^{u^\star}}\leq f_0$ **then**
12: Update $\mathbf{x}^u(n)$: $\mathbf{x}^u(n)\leftarrow\mathbf{x}^{u^\star}$
13: **else**
14: Keep $\mathbf{x}^u(n)$: $\mathbf{x}^u(n)\leftarrow\mathbf{x}^u(n-1)$
15: **end if**
16: Evaluate the objective function f_0 up to this point
17: Evaluate $\mathbf{x}^{d^\star}$ by solving problem (21) and using Algorithm 1
18: Evaluate the objective function with $\mathbf{x}^{d\star}$: $f_0|_{\mathbf{x}^{d^\star}}$
19: **if** $f_0|_{\mathbf{x}^{d^\star}}\leq f_0$ **then**
20: Update $\mathbf{x}^{d^n}$: $\mathbf{x}^{d^n}\leftarrow\mathbf{x}^{d^\star}$
21: **else**
22: Keep $\mathbf{x}^{d^n}$: $\mathbf{x}^{d^n}\leftarrow\mathbf{x}^{d^{n-1}}$
23: **end if**
24: Update $\{\rho_i^u(n),\rho_j^d(n)\}$ using equations (22)
25: Evaluate the objective function $f_0(n)$
26: **end while**
27: **Output**: $\mathbf{r}_i^u,r_j^d,\mathbf{w}_j^d,q_i^u,\mathbf{X}^u,\mathbf{X}^d$

V. Convergence and Complexity Analysis

To show the theoretical guarantees of our proposed solution, we establish the fundamental properties of Algorithm 2 in terms of convergence, complexity, and also specify how the necessary CSI is acquired.

A. Convergence

The convergence of the iterations in Algorithm 2 is established in Theorem 2. For sake of simplicity, we define $\boldsymbol{\pi}$ as the vector composed of all blocks, i.e., $\boldsymbol{\pi}=\big(\{\rho_i^u,\rho_j^d\},\{\mathbf{r}_i^u,r_j^d\},\{\mathbf{w}_j^d,q_i^u\},\{\mathbf{x}^u\},\{\mathbf{x}^d\}\big)$.

Theorem 2: Let $\{\boldsymbol{\pi}_n\}$ be the sequence generated by the updates of the variable $\boldsymbol{\pi}$ composed of all blocks generated by Algorithm 2. Then, the following is true:

1) The sequence of iterations $f(\{\boldsymbol{\pi}_n\})$ is non-increasing;
2) When the SDR in problem (21) is tight for both UL and DL blocks, $\{\boldsymbol{\pi}_n\}$ has limit points. Moreover, every limit point $\overline{\boldsymbol{\pi}}$ of $\{\boldsymbol{\pi}_n\}$ is a stationary point of the WMMSE objective function.

Proof: See Appendix G. ∎

Notice that part (a) of Theorem 2 is always guaranteed, and usually this condition is the best one can achieve when solving combinatorial problems within mixed-integer nonlinear problems. As for part (b), when the solution provided by SDR using randomization is tight, it guarantees that the iterates $\{\boldsymbol{\pi}_n\}$ converge to a stationary point. We note that the sufficient condition in Theorem 2 (b) is expected since globally optimal solution are needed to show BCD convergence. Thus, Theorem 2 ensures the convergence of Algorithm 2, and when randomization is tight, convergence to a stationary point.

B. Complexity

In the complexity analysis of Algorithm 2, we need to take into account the computational complexity of the blocks involved. We will neglect low complexity operations such as matrix multiplication, bisection, since their effect on the overall complexity is marginal. For the linear receiver blocks $\{\mathbf{r}_i^u(n), r_j^d(n)\}$ that are solved using equations (12a)-(12b), the most computationally demanding operation is the matrix inversion, which has overall complexity $\mathcal{O}\left(IM^3\right)$. For block $\{q_i^u(n)\}$ solved via equations (14)-(15), the overall complexity is dominated by the bisection, along with matrix and vector multiplications, which are all small. For block $\{\mathbf{w}_j^d(n)\}$ solved via equations (17)-(18), the complexity is dominated by the matrix inversion, which has complexity $\mathcal{O}(M^3)$.

For the assignment blocks $\{\mathbf{x}^u\}$ and $\{\mathbf{x}^d\}$, we analyse them as a single block because they have the same structure. Algorithm 2 solves the SDP problem (21) and later use randomization to retrieve a rank-1 solution. In the proposed SDP problem (21), the variable is matrix $\mathbf{Z}$, which is positive semidefinite and has $(M+1)(M+2)/2$ different entries, and has one constraint for each diagonal element $[\mathbf{Z}]_{nn}$. From [33], the complexity solving the SDP problem in (21) is $\mathcal{O}\left((M+1)^3(M+2)^2\right)$. For the randomization part, the most demanding operation is the Cholesky decomposition, which has complexity of $\mathcal{O}\left((M+1)^3\right)$ [34].

Therefore, from the above analysis the most demanding operation per iteration of Algorithm 2 is solving the SDP problem (21), which is much larger than all operations performed in other blocks. Disregarding terms of lower order, the worst-case complexity of Algorithm 2 is $\mathcal{O}(M^5)$.

C. CSI Acquisition

Algorithm 2 is centralized and run at the BS. The BS is the coordinator of the system and has knowledge of the CSI, which is also in accordance with some works in the full-duplex literature [19], [27]. We assume block fading channels, including the self-interference channels, the UL and DL channels, which remain unchanged during the coherence time. Therefore, our A-SDP solution in Algorithm 2 allows to find the near optimal antenna operation modes for a given channel setup.

TABLE I
SIMULATION PARAMETERS

Parameter	Value
Cell radius	$40\,\mathrm{m}$
Number of UL/DL UEs $[I = J]$	$[2\ 4]$
Number of antennas at BS M	$[4\ \ldots 64]$
Monte Carlo iterations	300
Carrier frequency / System bandwidth	$2.5\,\mathrm{GHz}/10\,\mathrm{MHz}$
LOS/NLOS path-loss model	Set according to [37, Table 6.2-1]
Shadowing st. dev. LOS/NLOS	$3\,\mathrm{dB}/4\,\mathrm{dB}$
Thermal noise power $[\sigma^2]$	$-174.4\,\mathrm{dBm/Hz}$
Noise figure BS/UL user	$13\,\mathrm{dB}/9\,\mathrm{dB}$
Tx/Rx distortions $[\kappa\ \beta]$	$[-120\ \ldots\ -50]$ dB (see [8], [20])
Residual SI power σ^2_{SI}	$[-100\ \ldots\ -50]$ dB
BS/UL user maximum power $(P^d_{\max}, P^u_{\max})$	$(30, 23)$ dBm

To acquire the channel gains, the BS transmits reference signals in the DL and receives them in UL, on which these signals are standardized by 3rd Generation Partnership Project (3GPP) [35]. For the SI channel, the estimates are obtained when using the SI suppression at the BS [2]. For the DL channel, the BS can use the reported received signal strength indicator (RSSI) or the reference signal receive power (RSRP) to estimate or measure the quality of the channel [35, Section 5.1.8]. For the UL channel, the users can transmit specific reference signals, such as the sounding reference signal (SRS), or the demodulation reference signal (DMRS) to enable the BS to acquire CSI. As for the interference channel between UL and DL users, the recently standardized measurement signals for device-to-device communications can be used, such as the sidelink transmission and reception reference signals [36]. The transmitter and receiver distortions in our model act as independent zero mean Gaussian noise [8], whose variance is linearly proportional to the intended transmit or receive signal at the antenna. Hence, the transceiver distortions do not need to be taken into account when estimating the channels because they are considered in the signal model as noise.

VI. NUMERICAL RESULTS AND DISCUSSION

In this section we consider a single cell system operating in the pico cell scenario [37]. The total number of antennas at the BS varies between $M = 4, \ldots, 64$, and the total number of served users are $I + J = \{4, 8\}$, where we assume that $I = J$. For the initial points to be assigned in our proposed A-SDP algorithm, we set the UL and DL powers equal to maximum, while the assignment variables are set such that all antennas are used for simultaneous UL and DL transmissions (shared mode).

We compare the performance of our proposed solution with that of three other algorithms:

1) **EXH**: Exhaustive search of problem (11), which analyses all possible 2^{2M} assignments with optimal linear beamformers, and selects the antenna assignment that gives the highest sum rate. This solution is the global optimal solution for problem (11);
2) **SPLIT**: Equal splitting of antennas between UL and DL, i.e., separates half of the antennas for transmission ($\mathbf{x}^d = [\mathbf{0}_{M/2}\ \ \mathbf{1}_{M/2}]^{\mathrm{T}}$) and half of the antennas

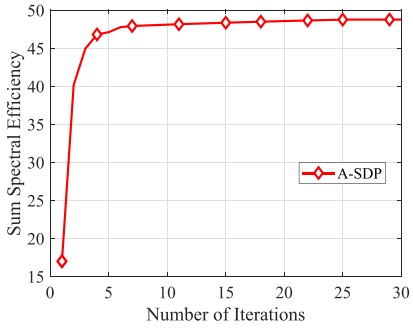

Fig. 3. Convergence rate of the proposed solution A-SDP with 4 antennas and 2 UL/DL users. Notice that the convergence is smooth is non-decreasing.

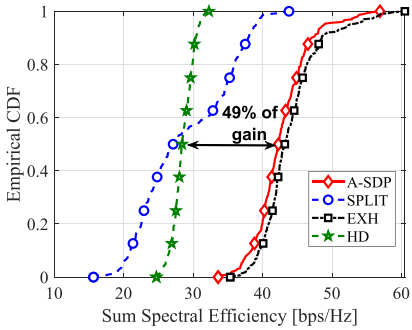

Fig. 4. Empirical CDF of the sum spectral efficiency of all users in a system with 4 antennas and 2 UL/DL users. The proposed A-SDP achieves a performance close to the exhaustive search EXH and better than SPLIT and HD.

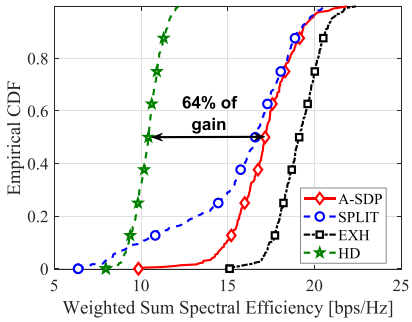

Fig. 5. Empirical CDF of the weighted sum spectral efficiency of all users in a system with 4 antennas and 2 UL/DL users, where the weights are the traffic asymmetry ($10-90\%$). The proposed A-SDP has a performance close to the exhaustive search EXH, and SPLIT reaches A-SDP at the 60-th percentile.

for reception ($\mathbf{x}^u = [\mathbf{1}_{M/2}\ \mathbf{0}_{M/2}]^{\mathrm{T}}$). Without loss of generality, we refer to the separate architecture as split in this section;

3) **HD**: Half-Duplex transmission, which uses the optimal linear beamformers achieved by solving the half-duplex version of problem (11) as in [10], i.e., without antenna assignment and coupling between UL and DL users. Moreover, either all antennas transmit (DL part) or all antennas receive (UL part).

In Section VI-A we show the convergence and optimality gap between our proposed algorithm against the exhaustive search of problem (11). For this, we also compare the performance of these algorithms when there is a traffic asymmetry between UL and DL. This is accomplished by setting the UL weights $\alpha_i^u = 0.1$ and DL weights $\alpha_j^d = 0.9$, which represent a traffic asymmetry of 10%-90% between UL and DL. In Section VI-B we compare the performance of these algorithms for different self-interference regime, number of UL/DL users, and Tx/Rx distortion. Furthermore, in Section VI-C we analyse the number of antennas and how the antennas are shared between UL/DL users in a system with small and high number of antennas.

A. Analysis of Optimality Gap

Figure 3 shows the convergence of A-SDP for a randomly selected Monte Carlo draw. The plot shows the sum spectral efficiency in a system with 4 antennas, 2 UL/DL users, and residual SI power of $\sigma_{\mathrm{SI}}^2 = -70$dB. As expected, the solution converges fast, in approximately 30 iterations, and the convergence is smooth and monotonically non-decreasing.

Using the same system configuration from Figure 3, we can now evaluate the performance of the proposed A-SDP with respect to EXH, SPLIT and HD. Figure 4 shows the empirical cumulative distribution function (CDF) of the sum spectral efficiency for all users, which is the objective function of problem (8). The optimality gap between A-SDP and EXH is negligible, while the sum spectral efficiency gain compared to HD is approximately 49% at the 50-th percentile. Moreover, SPLIT is worse than HD for approximately 54% of the cases, which shows that a naive splitting of the antennas is worse than HD solutions. In the Monte Carlo experiments in which SPLIT outperforms HD, UL and DL users in the system have better channel conditions than in the other Monte Carlo experiments. Overall, the gains of allowing antenna sharing – specifically through the proposed solution A-SDP – instead of the split solution is high, approximately 56% at the 50-th percentile.

To understand the impact of antenna splitting when the traffic is biased towards the DL, we set the weights $\alpha_i^u = 0.1$, $\alpha_j^d = 0.9$ to reflect the traffic asymmetry of 10% in the UL and 90% in the DL. Due to the non-convexity and combinatorial nature of our original problem (8), there are potentially many local minimum and saddle points. This suggests that we can initialize the power for the UL smaller than the maximum power for the traffic asymmetry case. In Figure 5 we notice that A-SDP has an optimality gap of approximately 10% with respect to EXH at the 50-th percentile. Interestingly, SPLIT reaches the same performance as A-SDP from the 60-th percentile onwards, which shows that a normal splitting of the antennas is the solution chosen in 40% of the cases by the close-to-optimal A-SDP. The gap between HD and A-SDP is approximately 64% at the 50-th percentile, while SPLIT outperforms HD only from the 9-th percentile onwards. Note that the main difference between SPLIT in Figures 4 and 5 is the point in which SPLIT outperforms HD. Due to the weights from the traffic asymmetry, it is expected that the objective function in the x-axis in Figure 5 is lower than Figure 4.

Engineering Insight 1: The proposed smart antenna architecture with a joint antenna assignment and beamforming design solution, named A-SDP, is close to the optimal solution

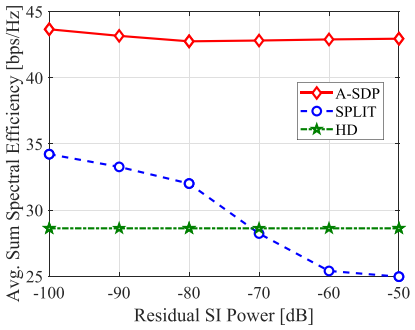

Fig. 6. Average sum spectral efficiency for different residual SI powers, assuming 4 antennas at the BS and 2 UL/DL users. The proposed A-SDP has almost no loss of performance across different residual SI powers. Moreover, SPLIT decreases quickly and is outperformed by HD.

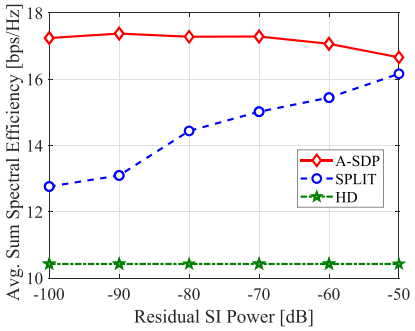

Fig. 7. Average weighted sum spectral efficiency for different residual SI powers, assuming 4 antennas at the BS and 2 UL/DL users. Once more, A-SDP maintains the average performance but now SPLIT improves with an increase in the residual SI power.

EXH, and greatly outperforms HD in terms of sum (and weighted sum) spectral efficiency with and without traffic bias. SPLIT reaches the same performance of A-SDP in many situations with traffic bias.

B. Analysis of the Self-Interference and Tx/Rx Distortions

In this section we present the average spectral efficiency for different residual SI powers and transceiver distortions. We vary the residual SI powers σ^2_{SI} from low (-100dB) to high (-50dB) residual SI power power. We analyse the impact of the number of UL/DL, and the Rician factor K in the sum spectral efficiency. For the transceiver distortions, we vary κ/β from low (-120dB) to high (-50dB) Tx/Rx distortions. Figure 6 shows the average sum spectral efficiency for a system with 4 antennas at the BS and 2 UL/DL users. Note that A-SDP maintains almost the same average spectral efficiency for high and low residual SI powers. Because of the antenna sharing, all UL and DL users have access to more antennas, which can be used to suppress SI. In contrast, SPLIT quickly decreases with an increase in the residual SI power, which is outperformed by HD from -70dB onwards.

Figure 7 shows the average weighted sum spectral efficiency with the same traffic asymmetry between UL and DL users as in the previous case, 10-90%. Similarly to Figure 6, the proposed A-SDP solution is able to maintain almost the same performance with different residual SI powers. Surprisingly, the SPLIT solution improves with high residual SI power. The reason is that the asymmetry prioritizes DL over UL transmissions, which are the ones impacted by SI. For this reason, the performance of the UL users are degraded more by SI, but since their priority is low, the system increases the spectral efficiency of DL users rather than reducing it in order to mitigate the impact of SI on the UL users.

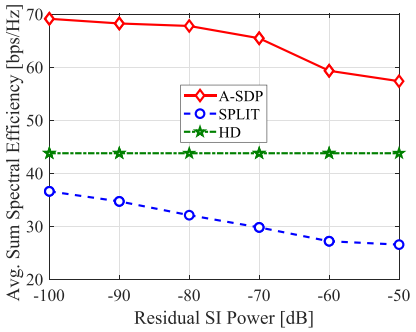

Fig. 8. Average sum spectral efficiency for different residual SI powers, assuming 4 antennas at the BS and 4 UL/DL users. With more users in the UL and DL, the antennas are no longer able to null more the self-interference, and thus the decrease with higher residual SI powers.

Engineering Insight 2: The proposed A-SDP solution is resilient against residual SI power, with or without traffic asymmetry. SPLIT outperforms HD and is close to the A-SDP solution when the residual SI power is high and with traffic asymmetry. Notably, the shared architecture, represented by our A-SDP solution, is more robust to residual SI power than the split architecture, represented by SPLIT.

Figure 8 shows the average sum spectral efficiency with 4 UL and DL users while maintaining 4 antennas at the BS. Notice that the proposed A-SDP solution decreases quickly with increasing residual SI power, but still outperforms HD. Since it is harder for the antenna assignment to select some antennas to be in only UL or only in DL because of the high number of users in the system, the beamforming is less effective in nulling the remaining SI with a higher number of spatially multiplexed users. Moreover, the SPLIT solution is worse than HD for all residual SI powers, showing that in scenarios with a high number of users this solution should not be selected.

Engineering Insight 3: With more users in the system, A-SDP solution still outperforms HD but its performance decreases quickly with an increase in the residual SI power. SPLIT is outperformed by HD for all the residual SI powers analysed. Specifically, spatially multiplexing high number of users brings performance degradation to the shared architecture, and much higher degradation to the split architecture.

To understand the impact of the Rician fading in our proposed solution A-SDP, we compare in Figure 9 the average spectral efficiency for $K = 30$dB and $K = 0$dB. When $K = 30$dB, the line of sight part of the SI channel dominates the channel, which implies that the SI channel has very few strong directions. Due to this reason, the average spectral efficiency barely changes for the A-SDP solution and increases for the SPLIT algorithm. For the A-SDP, the average

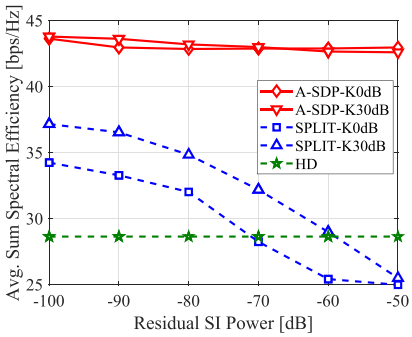

Fig. 9. Average sum spectral efficiency for different residual SI powers and Rician K factors, assuming 4 antennas at the BS and 2 UL/DL users. Notice that with $K = 30$dB, the average spectral efficiency increases significantly for the SPLIT solution but mildly for A-SDP.

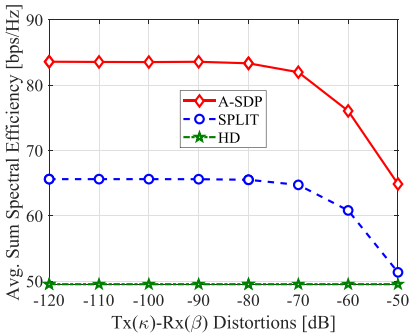

Fig. 10. Average sum spectral efficiency for different Tx and Rx distortions in a system with residual SI power of -70dB, assuming 8 antennas at the BS and 4 UL/DL users.

spectral efficiency is initially higher, the maximum relative gain reached is approximately 1.5% when the at -90dB of residual SI power. In addition, the curves for $K = 30$dB and 0dB cross-over at -70dB of residual SI power, and for $K = 30$dB the average relative loss with respect to $K = 0$dB is approximately 0.86% at -50dB of residual SI power. Thus, the impact of a higher Rician K factor in the A-SDP algorithm is negligible. The reason is that A-SDP is already using the antenna assignment to select the direction with the strongest eigenvalues and may decide to not use the weaker directions that will only create more SI. When comparing the Rician K factor for the SPLIT algorithm, the average spectral efficiency increases by approximately 8.5% with a residual SI power of -100dB. When the residual SI power reaches -50dB, which is a very strong SI signal, the difference is approximately 2%.

Engineering Insight 4: Scenarios with strong LOS conditions, i.e. high Rician factor K, strongly impact the performance of the SPLIT algorithm but mildly for the A-SDP algorithm. The A-SDP algorithm is already selecting the strongest eigenvalues (LOS direction) and may decide to not use the weaker directions.

Figure 10 shows the average sum spectral efficiency with 4 UL and DL users while maintaining 8 antennas at the BS. As the distortions at the Tx/Rx increase past -80dB, the sum spectral efficiency decreases sharply. Recall that in Figure 10 the total number of spatially multiplexed users is the same as the total number of antennas, and the decrease in sum spectral

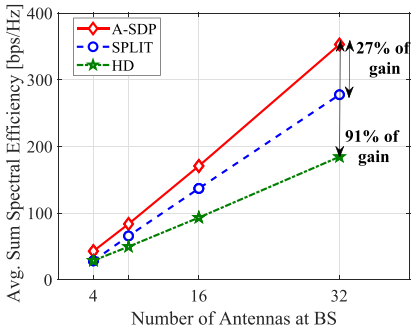

Fig. 11. Average sum spectral efficiency for number of antennas at the BS while maintaining the ration between antennas and users equals to two. Assuming a residual SI power of -70dB, the difference between A-SDP and SPLIT increases with the number of antennas, as well as the gains with respect to HD.

efficiency is still high with a high distortion. Comparing this result with Figure 7, the impact of Tx/Rx distortions is higher than the impact of high residual SI power.

Engineering Insight 5: The proposed solution A-SDP is resilient to high Tx/Rx distortion up to a certain power level, at which the sum spectral efficiency starts to decrease quickly. Moreover, the impact of high Tx/Rx distortion in the system is higher than high residual SI power.

C. Analysis of Number of Antennas

As the number of antennas at the BS increases, it becomes more difficult to implement the shared architecture due to the usage of analog circuits (circulators and duplexers) that are currently available. Nevertheless, it is important to understand the gains when antenna sharing is available for a high number of antennas, which yields a higher degree of freedom for the proposed antenna assignment solution A-SDP. Figure 11 shows the average sum spectral efficiency in a system with residual SI power of -70dB, and assuming a fixed ratio between antennas and UL/DL users equals to two. As the number of antennas and users in the system increases, notice that the gap between A-SDP and SPLIT widens and reaches 27% with 32 antennas. Moreover, the gains with respect to HD also increase with the number of antennas; using our proposed A-SDP solution the relative gain is approximately 91%. Therefore, if antenna sharing is available in the antenna assignment algorithm, the gains when compared to a simple split solution and HD are high.

Engineering Insight 6: With an increasing number of antennas and UL/DL users, A-SDP solution outperforms SPLIT and HD in terms of average sum spectral efficiency. Thus, it is advantageous to use the shared architecture for systems with high number of antennas and UL/DL users.

VII. Conclusion

In this article we considered the fundamentals of sharing and splitting of antennas in UL and DL of a base station in order to maximize the performance of full-duplex communications. Specifically, our objective was to show the benefits of a new smart antenna architecture. We investigated these benefits by the weighted sum spectral efficiency of UL and DL users in FD

cellular networks, which resulted in an NP-hard problem. Due to its inherent block nature of such a problem, we resorted to block coordinate descent to solve it in a per block manner. For the blocks with continuous variables, the problems were proved to be convex and the optimum solutions were provided. For the antenna assignment blocks, we proved that the problems are NP-hard, and we obtained a close-to-optimal solution using SDR with randomization. We also showed that the A-SDP solution monotonically increases the weighted sum spectral efficiency.

The numerical results demonstrated that our A-SDP solution improved the weighted sum spectral efficiency of the users when compared to a naive splitting of antennas and HD transmissions, while being close to the optimal exhaustive search. Moreover, our solution is robust against changes in the SI residual power, to changes in the Tx/Rx distortion up to a certain power level, and the gains with respect to the split solution and HD transmission increase with the number of antennas. Finally, the results show that a smart antenna assignment greatly outperforms a naive antenna splitting solution.

In future works, we intend to analyse the impact of antenna sharing and splitting in a system with multiple antennas also at the user side. Moreover, the time evolution of the UL and DL channels and fairness aspects on the proposed smart architecture are important directions that need further investigation.

Appendix A
Useful Properties

Throughout the article we need to use some properties related to the trace of a matrix, and the diagonal operator. We enumerate these properties below:

1) $\mathrm{tr}\left(\mathbf{AB}\right)=\mathrm{tr}\left(\mathbf{BA}\right)$;
2) $\mathbf{x}^H\mathbf{Ax}=\mathrm{tr}\left(\mathbf{x}^{\mathrm{H}}\mathbf{Ax}\right)=\mathrm{tr}\left(\mathbf{Axx}^{\mathrm{H}}\right)$;
3) $\sum_i \mathrm{tr}\left(\mathbf{x}^{\mathrm{H}}\mathbf{A}_i\mathbf{x}\right)=\mathrm{tr}\left(\mathbf{x}^{\mathrm{H}}\left(\sum_i \mathbf{A}_i\right)\mathbf{x}\right)$;
4) $\mathrm{tr}\left(\mathrm{diag}(\mathbf{xx}^{\mathrm{H}})\mathbf{A}\right)=\mathbf{x}^{\mathrm{H}}\,\mathrm{diag}(\mathbf{A})\mathbf{x}$;
5) $\mathbf{y}^{\mathrm{H}}\,\mathrm{diag}\left(\mathbf{x}\right)\mathbf{A}\,\mathrm{diag}\left(\mathbf{x}\right)\mathbf{z} = \mathbf{x}^{\mathrm{H}}\left(\mathrm{Diag}\left(\mathbf{y}^{\mathrm{H}}\right)\mathbf{A}\,\mathrm{Diag}\left(\mathbf{z}\right)\right)\mathbf{x}$.

Appendix B
Proof of Theorem 1

Our channel model can be understood as one SIMO interference broadcast channel in the UL and one MISO broadcast channel in the DL. Since both the SIMO and MISO broadcast channels are covered by the results in [10], our model that assumes a combination of both is also ensured by the results in [10].

For the equivalence for the transmit beamformers, $\mathbf{w}_j^d$, the transmit powers, q_i^u, and the receive beamformers, $\mathbf{r}_i^u$ and r_j^d, is established by Theorem 1 in [10]. The optimal weights ρ_i^u and ρ_j^d are found by checking first order optimality conditions, and are given by

$$\rho_i^u=(E_i^u)^{-1},\quad \rho_i^u=(E_j^d)^{-1}. \tag{22}$$

With respect to the antenna selection variables, $\mathbf{x}^u$ and $\mathbf{x}^d$, the equivalence is established when the variables are fixed. The proof of [10, Theorem 1] requires the variables to be continuous so that first order optimality can be used. Hence, since the antenna selection variables are binary, the equivalence established by [10, Theorem 1] can no longer be established if there are discrete variables in the optimization problem. For fixed antenna selection variables, all the remaining variables are continuous and the equivalence is established between problems (8) and (11) with the same fixed antenna selection variables. The equivalence between problems (8) and (11) is in the natural sense that the global optimal solutions to optimization variables $\mathbf{x}^u, \mathbf{x}^d$, $\{q_i^u\}, \{\mathbf{r}_i^u\}, \{\mathbf{w}_j^d\}, \{r_j^d\}$ for both problems are the same [38].

Appendix C
Proof of Proposition 1

Using Properties (1)-(4) in Appendix A, such as Properties (1)-(4), we define function $f^u(\{q_i^u\})$ as

$$f^u(\{q_i^u\})=\sum\nolimits_{i=1}^{I} f_i^u(q_i^u), \tag{23}$$
$$f_i^u(q_i^u)=\left(\delta_i^u+\mathrm{tr}\left(\Delta_i^u\mathbf{R}^u\right)\right)q_i^u-2\alpha_i^u\rho_i^u\,\mathrm{Re}\left\{\mathbf{r}_i^{u\mathrm{H}}\widetilde{\mathbf{h}^u}_i\right\}\sqrt{q_i^u}$$

where

$$\delta_i^u=(\kappa+\beta+1)\sum\nolimits_{j=1}^{J}\alpha_j^d\rho_j^d\left|r_j^d\right|^2\left|g_{ij}\right|^2, \tag{24a}$$
$$\mathbf{\Delta}_i^u=(1+\kappa)\widetilde{\mathbf{h}^u}_i\widetilde{\mathbf{h}_i^u}^{\mathrm{H}}+\beta\,\mathrm{diag}\left(\widetilde{\mathbf{h}^u}_l\widetilde{\mathbf{h}_l^u}^{\mathrm{H}}\right), \tag{24b}$$
$$\mathbf{R}^u=\sum\nolimits_{l=1}^{I}\alpha_l^u\rho_l^u\mathbf{r}_l^u\mathbf{r}_l^{u\mathrm{H}}. \tag{24c}$$

Using similar properties as before, we can write $f^d(\{\mathbf{w}_j^d\})$ as

$$f^d(\{\mathbf{w}_j^d\})=\sum\nolimits_{j=1}^{J}f_j^d(\mathbf{w}_j^d),$$
$$f_j^d(\mathbf{w}_j^d)=\mathbf{w}_j^d\mathbf{\Sigma}_j^d\mathbf{w}_j^{d\mathrm{H}}-2\alpha_j^d\rho_j^d\,\mathrm{Re}\left\{r_j^{d\mathrm{H}}\widetilde{\mathbf{h}_j^d}^{\mathrm{H}}\mathbf{w}_j^d\right\}, \tag{25}$$

where

$$\mathbf{\Sigma}_j^d=\widetilde{\mathbf{H}}_{\mathrm{SI}}^{\mathrm{H}}\left(\mathbf{R}^u+\beta\,\mathrm{diag}\left(\mathbf{R}^u\right)\right)\widetilde{\mathbf{H}}_{\mathrm{SI}}+\kappa\,\mathrm{diag}\left(\widetilde{\mathbf{H}}_{\mathrm{SI}}^{\mathrm{H}}\mathbf{R}^u\widetilde{\mathbf{H}}_{\mathrm{SI}}\right)+r^d\left((\beta+1)\widetilde{\mathbf{H}_j^d}+\kappa\,\mathrm{diag}(\widetilde{\mathbf{H}_j^d})\right), \tag{26a}$$
$$\widetilde{\mathbf{H}_j^d}=\widetilde{\mathbf{h}_j^d}\widetilde{\mathbf{h}_j^d}^{\mathrm{H}},\quad r^d=\sum\nolimits_{m=1}^{J}\alpha_m^d\rho_m^d\left|r_m^d\right|^2. \tag{26b}$$

Appendix D
Proof of Proposition 2

Initially, we define function $f^u(\mathbf{X}^u)$ as

$$f^u(\mathbf{X}^u)=\sum\nolimits_{i=1}^{I}\alpha_i^u\rho_i^u\Big\{\mathbf{r}_i^{u\mathrm{H}}\mathbf{X}^u\mathbf{\Gamma}_1^u\mathbf{X}^u\mathbf{r}_i^u+\sigma^2\mathbf{r}_i^{u\mathrm{H}}\mathbf{X}^u\mathbf{r}_i^u-2\sqrt{q_i^u}\,\mathrm{Re}\left\{\mathbf{r}_i^{u\mathrm{H}}\mathbf{X}^u\mathbf{h}_i^u\right\}\Big\}, \tag{27}$$

where $\mathbf{\Gamma}_1^u$ is defined as

$$\mathbf{\Gamma}_1^u=\sum\nolimits_{l=1}^{I}q_l^u\left[(\kappa+1)\mathbf{h}_l^u\mathbf{h}_l^{u\mathrm{H}}+\beta\,\mathrm{diag}\left(\mathbf{h}_l^u\mathbf{h}_l^{u\mathrm{H}}\right)\right]. \tag{28}$$

In addition, we define function $f^d(\mathbf{X}^d)$ as

$$f^d(\mathbf{X}^d)=\sum_{j=1}^{J}\left\{\mathbf{w}_j^{d\mathrm{H}}\mathbf{X}^d\mathbf{\Theta}_j^d\mathbf{X}^d\mathbf{w}_j^d-2\alpha_j^d\rho_j^d\,\mathrm{Re}\left\{r_j^{d\mathrm{H}}\mathbf{h}_j^{d\mathrm{H}}\mathbf{X}^d\mathbf{w}_j^d\right\}\right\}, \tag{29}$$

where

$$\mathbf{\Theta}_j^d = r^d(\beta+1)\mathbf{H}_j^d + r^d\kappa\,\mathrm{diag}\left(\mathbf{H}_j^d\right). \tag{30}$$

Finally, we define

$$\begin{aligned} f^{u,d}(\mathbf{X}^u,\mathbf{X}^d) &= \sum\nolimits_{i=1}^{I}\sum\nolimits_{j=1}^{J}\alpha_i^u\rho_i^u\mathbf{r}_i^{u\mathrm{H}}\Big\{\mathbf{X}^u\mathbf{H}_{\mathrm{SI}}\mathbf{X}^d\Big(\mathbf{w}_j^d\mathbf{w}_j^{d\mathrm{H}} \\ &\quad + \kappa\,\mathrm{diag}\left(\mathbf{w}_j^d\mathbf{w}_j^{d\mathrm{H}}\right)\Big)\mathbf{X}^d\mathbf{H}_{\mathrm{SI}}{}^{\mathrm{H}}\mathbf{X}^u \\ &\quad + \beta\,\mathrm{diag}\left(\mathbf{X}^u\mathbf{H}_{\mathrm{SI}}\mathbf{X}^d\mathbf{w}_j^d\mathbf{w}_j^{d\mathrm{H}}\mathbf{X}^d\mathbf{H}_{\mathrm{SI}}{}^{\mathrm{H}}\mathbf{X}^u\right)\Big\}\mathbf{r}_i^u. \end{aligned} \tag{31}$$

Since the UL block depends only on $\mathbf{X}^u$, we consider $f^{u,d}(\mathbf{X}^u,\mathbf{X}^d)$ with fixed $\mathbf{X}^d$, whereas the same applies for the DL block. Using the trace properties mentioned in Appendix A, we can write the updated expressions as

$$f^{u,d}(\mathbf{X}^u,\mathbf{X}^d)|_{\mathbf{X}^d\text{fix}} = \sum\nolimits_{i=1}^{I}\alpha_i^u\rho_i^u\mathbf{r}_i^{u\mathrm{H}}\mathbf{X}^u\mathbf{\Gamma}_2^u\mathbf{X}^u\mathbf{r}_i^u, \tag{32a}$$

$$\begin{aligned} f^{u,d}(\mathbf{X}^u,\mathbf{X}^d)|_{\mathbf{X}^u\text{fix}} &= \sum\nolimits_{j=1}^{J}\mathbf{w}_j^{d\mathrm{H}}\mathbf{X}^d\Big(\mathbf{\Gamma}_1^d + \kappa\,\mathrm{diag}(\mathbf{\Gamma}_1^d) \\ &\quad + \beta\mathbf{\Gamma}_2^d\Big)\mathbf{X}^d\mathbf{w}_j^d, \end{aligned} \tag{32b}$$

where matrices $\mathbf{\Gamma}_2^u, \mathbf{\Gamma}_1^d, \mathbf{\Gamma}_2^d$ are defined as

$$\begin{aligned} \mathbf{\Gamma}_2^u = \sum_{m=1}^{J}\Bigg[&\mathbf{H}_{\mathrm{SI}}\mathbf{X}^d\left(\mathbf{w}_m^d\mathbf{w}_m^{d\ \mathrm{H}} + \kappa\,\mathrm{diag}\left(\mathbf{w}_m^d\mathbf{w}_m^{d\ \mathrm{H}}\right)\right)\mathbf{X}^d\mathbf{H}_{\mathrm{SI}}{}^{\mathrm{H}} \\ &+\beta\,\mathrm{diag}\left(\mathbf{H}_{\mathrm{SI}}\mathbf{X}^d\mathbf{w}_m^d\mathbf{w}_m^{d\ \mathrm{H}}\mathbf{X}^d\mathbf{H}_{\mathrm{SI}}{}^{\mathrm{H}}\right)\Bigg], \end{aligned} \tag{33a}$$

$$\mathbf{\Gamma}_1^d = \mathbf{H}_{\mathrm{SI}}{}^{\mathrm{H}}\mathbf{X}^u\mathbf{R}^u\mathbf{X}^u\mathbf{H}_{\mathrm{SI}}, \tag{33b}$$

$$\mathbf{\Gamma}_2^d = \mathbf{H}_{\mathrm{SI}}{}^{\mathrm{H}}\mathbf{X}^u\,\mathrm{diag}\left(\mathbf{R}^u\right)\mathbf{X}^u\mathbf{H}_{\mathrm{SI}}. \tag{33c}$$

With these expressions, we can write the objective functions $\widetilde{f^u}(\mathbf{X}^u) = f^u(\mathbf{X}^u) + f^{u,d}(\mathbf{X}^u,\mathbf{X}^d)|_{\mathbf{X}^d\text{fix}}$ for UL, and $\widetilde{f^d}(\mathbf{X}^d) = f^d(\mathbf{X}^d) + f^{u,d}(\mathbf{X}^u,\mathbf{X}^d)|_{\mathbf{X}^u\text{fix}}$ for DL as

$$\begin{aligned} \widetilde{f^u}(\mathbf{X}^u) = \sum\nolimits_{i=1}^{I}\alpha_i^u\rho_i^u\Big\{&\mathbf{r}_i^{u\mathrm{H}}\mathbf{X}^u\mathbf{\Lambda}^u\mathbf{X}^u\mathbf{r}_i^u + \sigma^2\mathbf{r}_i^{u\mathrm{H}}\mathbf{X}^u\mathbf{r}_i^u \\ &- 2\sqrt{q_i^u}\,\mathrm{Re}\left\{\mathbf{r}_i^{u\mathrm{H}}\mathbf{X}^u\mathbf{h}_i^u\right\}\Big\}, \end{aligned} \tag{34a}$$

$$\widetilde{f^d}(\mathbf{X}^d) = \sum_{j=1}^{J}\left\{\mathbf{w}_j^{d\mathrm{H}}\mathbf{X}^d\mathbf{\Lambda}_j^d\mathbf{X}^d\mathbf{w}_j^d - 2\alpha_j^d\rho_j^d\,\mathrm{Re}\left\{r_j^{d\mathrm{H}}\mathbf{h}_j^{d\mathrm{H}}\mathbf{X}^d\mathbf{w}_j^d\right\}\right\}, \tag{34b}$$

where matrices $\mathbf{\Lambda}^u,\ \mathbf{\Lambda}_j^d$ are defined as

$$\mathbf{\Lambda}^u = \mathbf{\Gamma}_1^u + \mathbf{\Gamma}_2^u, \tag{35a}$$

$$\mathbf{\Lambda}_j^d = \mathbf{\Theta}_j^d + \mathbf{\Gamma}_1^d + \kappa\,\mathrm{diag}(\mathbf{\Gamma}_1^d) + \mathbf{\Gamma}_2^d. \tag{35b}$$

APPENDIX E
PROOF OF PROPOSITION 3

Since the expressions for UL and DL have similar structure, we will prove only for the DL. Then, using Property 5 from Appendix A, we can write the quadratic term with $\mathbf{X}^d$ as

$$\begin{aligned} \sum_{j=1}^{J}\mathbf{w}_j^{d\mathrm{H}}\mathbf{X}^d\mathbf{\Lambda}_j^d\mathbf{X}^d\mathbf{w}_j^d &= \mathbf{x}^{d\mathrm{T}}\left(\sum_{j=1}^{J}\mathrm{diag}\left(\mathbf{w}_j^{d\mathrm{H}}\right)\mathbf{\Lambda}_j^d\mathrm{diag}\left(\mathbf{w}_j^d\right)\right)\mathbf{x}^d, \\ &= \mathbf{x}^{d\mathrm{T}}\widetilde{\mathbf{\Lambda}^d}\mathbf{x}^d, \end{aligned} \tag{36}$$

where

$$\widetilde{\mathbf{\Lambda}^d} = \sum\nolimits_{j=1}^{J}\mathrm{diag}\left(\mathbf{w}_j^{d\mathrm{H}}\right)\mathbf{\Lambda}_j^d\,\mathrm{diag}\left(\mathbf{w}_j^d\right). \tag{37}$$

Using Property 1 for the linear term on $\mathbf{X}^d$, we have that

$$\begin{aligned} \mathrm{Re}\left\{r_j^{d\mathrm{H}}\mathbf{h}_j^{d\mathrm{H}}\mathbf{X}^d\mathbf{w}_j^d\right\} &= \mathrm{Re}\left\{r_j^{d\mathrm{H}}\,\mathrm{tr}\left(\mathbf{h}_j^{d\mathrm{H}}\,\mathrm{diag}\left(\mathbf{x}^d\right)\mathbf{w}_j^d\right)\right\}, \\ &= \mathrm{Re}\left\{r_j^{d\mathrm{H}}\,\mathrm{tr}\left(\mathrm{diag}\left(\mathbf{x}^d\right)\mathbf{w}_j^d\mathbf{h}_j^{d\mathrm{H}}\right)\right\}, \\ &= \mathrm{Re}\left\{r_j^{d\mathrm{H}}\mathrm{Diag}\left(\mathbf{h}_j^d\mathbf{w}_j^{d\mathrm{H}}\right)\mathbf{x}^d\right\}, \end{aligned} \tag{38}$$

and by including the full term with the sum, we obtain

$$\sum\nolimits_{j=1}^{J}\alpha_j^d\rho_j^d\,\mathrm{Re}\left\{r_j^{d\mathrm{H}}\mathrm{Diag}\left(\mathbf{h}_j^d\mathbf{w}_j^{d\mathrm{H}}\right)\right\}\mathbf{x}^d = \mathbf{a}^{d\mathrm{T}}\mathbf{x}^d, \tag{39}$$

where $\mathbf{a}^d$ is defined as

$$\mathbf{a}^d = \sum\nolimits_{j=1}^{J}\alpha_j^d\rho_j^d\,\mathrm{Re}\left\{r_j^{d\mathrm{H}}\mathrm{Diag}\left(\mathbf{h}_j^d\mathbf{w}_j^{d\mathrm{H}}\right)\right\}. \tag{40}$$

Thus, we can write $\widetilde{f^d}(\mathbf{X}^d)$ in equation (34b) in the equivalent form as

$$\begin{aligned} \widetilde{f^d}(\mathbf{X}^d) &= \sum_{j=1}^{J}\left\{\mathbf{w}_j^{d\mathrm{H}}\mathbf{X}^d\mathbf{\Lambda}_j^d\mathbf{X}^d\mathbf{w}_j^d - 2\alpha_j^d\rho_j^d\,\mathrm{Re}\left\{r_j^{d\mathrm{H}}\mathbf{h}_j^{d\mathrm{H}}\mathbf{X}^d\mathbf{w}_j^d\right\}\right\}, \\ &= \mathbf{x}^{d\mathrm{T}}\widetilde{\mathbf{\Lambda}^d}\mathbf{x}^d - 2\mathbf{a}^{d\mathrm{T}}\mathbf{x}^d. \end{aligned} \tag{41}$$

The UL expression for $\widetilde{f^u}(\mathbf{X}^u)$ can be written in a similar form, but using matrix $\widetilde{\mathbf{\Lambda}^u}$ and vector $\mathbf{a}^u$, which are defined as

$$\widetilde{\mathbf{\Lambda}^u} = \sum\nolimits_{i=1}^{I}\alpha_i^u\rho_i^u\,\mathrm{diag}\left(\mathbf{r}_i^{u\mathrm{H}}\right)\mathbf{\Lambda}^u\,\mathrm{diag}\left(\mathbf{r}_i^u\right), \tag{42a}$$

$$\begin{aligned} \mathbf{a}^u = \sum\nolimits_{i=1}^{I}\alpha_i^u\rho_i^u\Bigg\{&\sqrt{q_i^u}\,\mathrm{Re}\left\{\mathrm{Diag}\left(\mathbf{r}_i^u\mathbf{h}_i^{u\mathrm{H}}\right)^{\mathrm{H}}\right\} \\ &- \frac{\sigma^2}{2}\mathrm{Diag}\left(\mathbf{r}_i^u\mathbf{r}_i^{u\mathrm{H}}\right)\Bigg\}. \end{aligned} \tag{42b}$$

Therefore, we write problem (19) in an equivalent non-homogeneous quadratic problem as

$$\underset{\mathbf{x}}{\text{minimize}}\ \mathbf{x}^{\mathrm{T}}\widetilde{\mathbf{\Lambda}}\mathbf{x} - 2\mathbf{a}^{\mathrm{T}}\mathbf{x} \tag{43a}$$

$$\text{subject to } x_k \in \{0,1\},\quad \forall k = 1,\ldots,M. \tag{43b}$$

In order to write problem (43) into an homogeneous quadratic problem, the first step is to convert the binary vector $\mathbf{x}$ into the boolean vector $\mathbf{v}$, where $\mathbf{v} = 2\mathbf{x} - \mathbf{1}$ and $\mathbf{x} = (1/2)(\mathbf{v}+\mathbf{1})$. With this, the problem (43) can be written into the boolean equivalent formulation:

$$\underset{\mathbf{v}}{\text{minimize}}\ \frac{1}{4}\mathbf{v}^{\mathrm{T}}\widetilde{\mathbf{\Lambda}}\mathbf{v} - \mathbf{b}^{\mathrm{T}}\mathbf{v} + d \tag{44a}$$

$$\text{subject to } v_k \in \{-1,1\},\ \forall k = 1,\ldots,M, \tag{44b}$$

where the vector $\mathbf{b}$ and scalar d are defined as $\mathbf{b} = \mathbf{a} - \frac{1}{2}\,\mathrm{Re}\left\{\mathbf{1}^{\mathrm{T}}\widetilde{\mathbf{\Lambda}}\right\}$, and $d = \left(\frac{1}{4}\mathbf{1}^{\mathrm{T}}\widetilde{\mathbf{\Lambda}}\mathbf{1} - \mathbf{a}^{\mathrm{T}}\mathbf{1}\right)$.

The next step is to convert the objective function in Eq. (44a) into an homogeneous quadratic function, and to do this we follow the steps in [12]. Let us define the boolean scalar $t \in \{\pm 1\}$, which implies that $t^2 = 1$. Then, we define the auxiliary variable $\tilde{\mathbf{v}}$, such that $\mathbf{v} = t\tilde{\mathbf{v}}$. With the change of variables, problem (44) becomes:

$$\underset{\tilde{\mathbf{v}},t}{\text{minimize}}\ \frac{1}{4}\tilde{\mathbf{v}}^{\mathrm{T}}\widetilde{\mathbf{\Lambda}}\tilde{\mathbf{v}} - \mathbf{b}^{\mathrm{T}}t\tilde{\mathbf{v}} + d \tag{45a}$$

$$\text{subject to } t, \tilde{v}_k \in \{-1, 1\},\ \forall k = 1, \ldots, M, \tag{45b}$$

Then, consider the vector $\mathbf{z}$ and matrix $\mathbf{\Upsilon}$ defined as

$$\mathbf{z} = \begin{bmatrix} \tilde{\mathbf{v}} & t \end{bmatrix}^{\mathrm{T}} \in \{\pm 1\}^{M+1}, \tag{46a}$$

$$\mathbf{\Upsilon} = \begin{bmatrix} (1/4)\widetilde{\mathbf{\Lambda}} & -\mathbf{b}/2 \\ -\mathbf{b}^{\mathrm{T}}/2 & 0_{1\times 1} \end{bmatrix}. \tag{46b}$$

Using $\mathbf{z}$ and matrix $\mathbf{\Upsilon}$, we can write the objective function (45a) as an homogeneous quadratic function

$$\frac{1}{4}\mathbf{v}^{\mathrm{T}}\widetilde{\mathbf{\Lambda}}\mathbf{v} - \mathbf{b}^{\mathrm{T}}\mathbf{v} + d = \mathbf{z}^{\mathrm{T}}\mathbf{\Upsilon}\mathbf{z} + d. \tag{47}$$

With this, we can now write problem (19) as the homogeneous boolean quadratic problem defined in (20).

Appendix F
Proof of Proposition 4

In the following, we use Property 2 to arrive into an SDP function as

$$\mathbf{z}^{\mathrm{T}}\mathbf{\Upsilon}\mathbf{z} = \mathrm{tr}\left(\mathbf{z}^{\mathrm{T}}\mathbf{\Upsilon}\mathbf{z}\right) = \mathrm{tr}\left(\mathbf{\Upsilon}\underbrace{\mathbf{z}\mathbf{z}^{\mathrm{T}}}_{\mathbf{Z}}\right) = \mathrm{tr}\left(\mathbf{\Upsilon}\mathbf{Z}\right). \tag{48}$$

With the new matrix $\mathbf{Z}$ as variable, we replace constraint (45b) by $[\mathbf{Z}]_{nn} = 1$ for all the diagonal elements, and add two new constraints: matrix $\mathbf{Z}$ needs to be positive semidefinite, i.e., $\mathbf{Z} \succeq \mathbf{0}$; and the rank of $\mathbf{Z}$ needs to be equal to one, i.e., $\mathrm{rank}\,(\mathbf{Z}) = 1$. Applying these modifications, we rewrite problem (45) into the SDP equivalent form as

$$\underset{\mathbf{Z}}{\text{minimize}}\ \mathrm{tr}\,(\mathbf{\Upsilon}\mathbf{Z}) + d \tag{49a}$$

$$\text{subject to } [\mathbf{Z}]_{nn} = 1, n = 1, \ldots, M+1, \tag{49b}$$

$$\mathrm{rank}\,(\mathbf{Z}) = 1, \tag{49c}$$

$$\mathbf{Z} \succeq \mathbf{0}. \tag{49d}$$

Problem (49) is equivalent to the initial problem (43), i.e., they yield the same optimal solution [38]. Although matrix $\mathbf{Z}$ does not need to be boolean, the rank-1 constraint (49c) makes the problem non-convex and NP-hard [12]. To circumvent this difficulty, we relax the rank-1 constraint (49c), and write the SDR formulation as defined in problem (21).

Appendix G
Proof of Theorem 2

The proof of part (a) follows from the BCD approach. For blocks $\{\rho_i^u, \rho_j^d\}, \{\mathbf{r}_i^u, r_j^d\}, \{\mathbf{w}_j^d, q_i^u\}$, the objective function minimized at each block iteration is strictly convex. Thus, these blocks have a unique minimizer and the iterations provide a non-increasing objective function at every iteration. For blocks $\{\mathbf{x}^u\}, \{\mathbf{x}^d\}$, the SDR provides an approximate solution to problem (20), which is in the direction of the optimal solution for the SDR problem (21). Although the approximated solution is in the direction of the minimizer, we update the blocks only if the objective function is not increased in Algorithm 2. Therefore, the iterations provided by Algorithm 2 are non-increasing.

For part (b), we find useful to have some definitions. Let us define the general constraint set $\mathbf{\Pi}$ as the Cartesian product of all the constraint sets of all blocks. Since the SDR is now tight for both UL and DL blocks, we can consider the constraint set of the SDR problem (21) instead of the original discrete constraint set of problem (20). We denote by $\mathcal{L}_{\boldsymbol{\pi}}^0$ the level set of the WMMSE objective function in problem (8a) $f(\boldsymbol{\pi})$ relative to $\mathbf{\Pi}$, corresponding to a given point $\boldsymbol{\pi}^0 \in \mathbf{\Pi}$, that is $\mathcal{L}_{\boldsymbol{\pi}}^0 \triangleq \{\boldsymbol{\pi} \in \mathbf{\Pi} : f(\boldsymbol{\pi}) \leq f(\boldsymbol{\pi}^0)\}$. Then, for all blocks, the respective objective function is either convex or strictly convex. Moreover, the level set $\mathbf{\Pi}$ is closed in the domains of all variables in the blocks. Therefore, from [11, Proposition 5], part (b) follows.

Acknowledgment

The simulations were performed on resources provided by the Swedish National Infrastructure for Computing (SNIC) at PDC Centre for High Performance Computing (PDC-HPC).

References

[1] A. Sabharwal, P. Schniter, D. Guo, D. W. Bliss, S. Rangarajan, and R. Wichman, "In-band full-duplex wireless: Challenges and opportunities," *IEEE J. Sel. Areas Commun.*, vol. 32, no. 9, pp. 1637–1652, Sep. 2014.

[2] Z. Zhang, K. Long, A. V. Vasilakos, and L. Hanzo, "Full-duplex wireless communications: Challenges, solutions, and future research directions," *Proc. IEEE*, vol. 104, no. 7, pp. 1369–1409, Jul. 2016.

[3] J. M. B. da Silva, G. Fodor, and C. Fischione, "Fast-Lipschitz power control and user-frequency assignment in full-duplex cellular networks," *IEEE Trans. Wireless Commun.*, vol. 16, no. 10, pp. 6672–6687, Oct. 2017.

[4] M. Duarte, C. Dick, and A. Sabharwal, "Experiment-driven characterization of full-duplex wireless systems," *IEEE Trans. Wireless Commun.*, vol. 11, no. 12, pp. 4296–4307, Dec. 2012.

[5] D. Bharadia, E. McMilin, and S. Katti, "Full duplex radios," *SIGCOMM Comput. Commun. Rev.*, vol. 43, no. 4, pp. 375–386, Oct. 2013.

[6] M. Heino *et al.*, "Recent advances in antenna design and interference cancellation algorithms for in-band full duplex relays," *IEEE Commun. Mag.*, vol. 53, no. 5, pp. 91–101, May 2015.

[7] D. Korpi *et al.*, "Full-duplex mobile device: Pushing the limits," *IEEE Commun. Mag.*, vol. 54, no. 9, pp. 80–87, Sep. 2016.

[8] B. P. Day, A. R. Margetts, D. W. Bliss, and P. Schniter, "Full-duplex MIMO relaying: Achievable rates under limited dynamic range," *IEEE J. Sel. Areas Commun.*, vol. 30, no. 8, pp. 1541–1553, Sep. 2012.

[9] P. Belotti, C. Kirches, S. Leyffer, J. Linderoth, J. Luedtke, and A. Mahajan, "Mixed-integer nonlinear optimization," *Acta Numerica*, vol. 22, pp. 1–131, May 2013.

[10] Q. Shi, M. Razaviyayn, Z.-Q. Luo, and C. He, "An iteratively weighted MMSE approach to distributed sum-utility maximization for a MIMO interfering broadcast channel," *IEEE Trans. Signal Process.*, vol. 59, no. 9, pp. 4331–4340, Sep. 2011.

[11] L. Grippo and M. Sciandrone, "On the convergence of the block nonlinear Gauss–Seidel method under convex constraints," *Oper. Res. Lett.*, vol. 26, no. 3, pp. 127–136, Apr. 2000.

[12] Z.-Q. Luo, W.-K. Ma, A. So, Y. Ye, and S. Zhang, "Semidefinite relaxation of quadratic optimization problems," *IEEE Signal Process. Mag.*, vol. 27, no. 3, pp. 20–34, May 2010.

[13] D. Kim, H. Lee, and D. Hong, "A survey of in-band full-duplex transmission: From the perspective of PHY and MAC layers," *IEEE Commun. Surveys Tuts.*, vol. 17, no. 4, pp. 2017–2046, 4th Quart., 2015.

[14] E. Aryafar *et al.*, "MIDU: Enabling MIMO full duplex," in *Proc. Annu. Int. Conf. Mobile Comput. Netw. (Mobicom)*, 2012, pp. 257–268.

[15] M. Duarte *et al.*, "Design and characterization of a full-duplex multi-antenna system for WiFi networks," *IEEE Trans. Veh. Technol.*, vol. 63, no. 3, pp. 1160–1177, Mar. 2014.

[16] D. Korpi, M. Heino, C. Icheln, K. Haneda, and M. Valkama, "Compact inband full-duplex relays with beyond 100 dB self-interference suppression: Enabling techniques and field measurements," *IEEE Trans. Antennas Propag.*, vol. 65, no. 2, pp. 960–965, Feb. 2017.

[17] D. Bharadia and S. Katti, "Full duplex MIMO radios," in *Proc. USENIX Conf. Networked Syst. Design Implement. (NSDI)*, 2014, pp. 359–372.

[18] J. Zhou *et al.*, "Integrated full duplex radios," *IEEE Commun. Mag.*, vol. 55, no. 4, pp. 142–151, Apr. 2017.

[19] D. Nguyen, L.-N. Tran, P. Pirinen, and M. Latva-Aho, "On the spectral efficiency of full-duplex small cell wireless systems," *IEEE Trans. Wireless Commun.*, vol. 13, no. 9, pp. 4896–4910, Sep. 2014.

[20] A. C. Cirik, O. Taghizadeh, L. Lampe, R. Mathar, and Y. Hua, "Linear transceiver design for full-duplex multi-cell MIMO systems," *IEEE Access*, vol. 4, pp. 4678–4689, 2016.

[21] J. Kim, W. Choi, and H. Park, "Beamforming for full-duplex multi-user MIMO systems," *IEEE Trans. Veh. Technol.*, vol. 66, no. 3, pp. 2423–2432, Mar. 2017.

[22] M. Ahn, H.-B. Kong, H. M. Shin, and I. Lee, "A low complexity user selection algorithm for full-duplex MU-MISO systems," *IEEE Trans. Wireless Commun.*, vol. 15, no. 11, pp. 7899–7907, Nov. 2016.

[23] M. Zhou, H. Cui, L. Song, and B. Jiao, "Transmit-receive antenna pair selection in full duplex systems," *IEEE Wireless Commun. Lett.*, vol. 3, no. 1, pp. 34–37, Feb. 2014.

[24] E. Everett, C. Shepard, L. Zhong, and A. Sabharwal, "SoftNull: Many-antenna full-duplex wireless via digital beamforming," *IEEE Trans. Wireless Commun.*, vol. 15, no. 12, pp. 8077–8092, Dec. 2016.

[25] N. M. Gowda and A. Sabharwal, "JointNull: Combining partial analog cancellation with transmit beamforming for large-antenna full-duplex wireless systems," *IEEE Trans. Wireless Commun.*, vol. 17, no. 3, pp. 2094–2108, Mar. 2018.

[26] J. M. B. da Silva, Jr., H. Ghauch, G. Fodor, and C. Fischione, "How to split UL/DL antennas in full-duplex cellular networks," in *Proc. IEEE Int. Conf. Commun. Workshops (ICC Workshops)*, May 2018, pp. 1–6.

[27] A. C. Cirik, L. Zhou, and T. Ratnarajah, "Linear transceiver design with per-antenna power constraints in full-duplex multi-user MIMO systems," *IEEE Wireless Commun. Lett.*, vol. 5, no. 4, pp. 412–415, Aug. 2016.

[28] A. Hjørungnes, *Complex-Valued Matrix Derivatives: With Applications in Signal Processing and Communications*. Cambridge, U.K.: Cambridge Univ. Press, 2011.

[29] P. M. Pardalos and S. Jha, "Complexity of uniqueness and local search in quadratic 0–1 programming," *Oper. Res. Lett.*, vol. 11, no. 2, pp. 119–123, 1992.

[30] P. Hui Tan and L. K. Rasmussen, "The application of semidefinite programming for detection in CDMA," *IEEE J. Sel. Areas Commun.*, vol. 19, no. 8, pp. 1442–1449, Aug. 2001.

[31] W.-K. Ma, T. N. Davidson, K. M. Wong, Z.-Q. Luo, and P.-C. Ching, "Quasi-maximum-likelihood multiuser detection using semi-definite relaxation with application to synchronous CDMA," *IEEE Trans. Signal Process.*, vol. 50, no. 4, pp. 912–922, Apr. 2002.

[32] M. Kisialiou and Z.-Q. Luo, "Probabilistic analysis of semidefinite relaxation for binary quadratic minimization," *SIAM J. Optim.*, vol. 20, no. 4, pp. 1906–1922, Jan. 2010.

[33] M. S. Lobo, L. Vandenberghe, S. Boyd, and H. Lebret, "Applications of second-order cone programming," *Linear Algebra its Appl.*, vol. 284, nos. 1–3, pp. 193–228, Nov. 1998.

[34] R. Hunger, "Floating point operations in matrix-vector calculus," Technische Universität München, Munich, Germany, Tech. Rep., 2007. [Online]. Available: https://mediatum.ub.tum.de/doc/625604

[35] *Evolved Universal Terrestrial Radio Access (E-UTRA) and Evolved Universal Terrestrial Radio Access Network (E-UTRAN); Overall Description; Stage 2*, document TS 36.300, 3rd Generation Partnership Project (3GPP), Mar. 2017.

[36] *Evolved Universal Terrestrial Radio Access (E-UTRA) and Evolved Universal Terrestrial Radio Access Network (E-UTRAN); Physical Layer Procedures*, document TS 36.213, 3rd Generation Partnership Project (3GPP), Mar. 2017.

[37] *Evolved Universal Terrestrial Radio Access (E-UTRA); Further Enhancements to LTE Time Division Duplex (TDD) for Downlink-Uplink (DL-UL) Interference Management and Traffic Adaptation*, document TR 36.828, 3rd Generation Partnership Project (3GPP), Jun. 2012.

[38] S. Boyd and L. Vandenberghe, *Convex Optimization*. Cambridge, U.K.: Cambridge Univ. Press, 2004.

José Mairton B. da Silva, Jr. (Member, IEEE) received the B.Sc. (Hons.) and M.Sc. degrees in telecommunications engineering from the Federal University of Ceará, Fortaleza, Brazil, in 2012 and 2014, respectively, and the Ph.D. degree in electrical engineering and computer science from the KTH Royal Institute of Technology, Stockholm, Sweden, in 2019. From July 2012 to March 2015, he was a Research Engineer with the Wireless Telecommunication Research Group (GTEL), Fortaleza. From autumn/winter 2013 to 2014, he worked in an internship at Ericsson Research, Stockholm. In Spring/Fall 2018, he was a Visiting Researcher with Rice University, TX, USA. He is currently a Postdoctoral Researcher with the KTH Royal Institute of Technology. His research interests include distributed machine learning and optimization over wireless communications. He is also the Secretary of the IEEE Communications Society Emerging Technology Initiative on Full Duplex Communications.

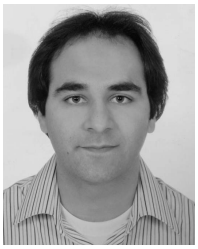

Hadi Ghauch (Member, IEEE) received the M.Sc. degree from Carnegie Mellon University, Pittsburgh, PA, USA, in 2011, and the Ph.D. degree in electrical engineering from the KTH Royal Institute of Technology, Stockholm, Sweden, in 2017. Since 2018, he has been an Assistant Professor with the Department of Digital Communications, Telecom-Paris Tech, and also with the Institut Polytechnique de Paris. His research interests include optimization for large-scale learning, optimization for millimeter-wave communication, and the distributed optimization of wireless networks.

Gábor Fodor (Senior Member, IEEE) received the Ph.D. degree in electrical engineering from the Budapest University of Technology and Economics in 1998 and the D.Sc. degree from the Hungarian Academy of Sciences (Doctor of MTA) in 2019. He is currently a Master Researcher with Ericsson Research and also a Docent and an Adjunct Professor with the KTH Royal Institute of Technology, Stockholm, Sweden. He has authored or coauthored more than 100 refereed journal articles and conference articles and seven book chapters and holds more than 100 European and U.S. granted patents.

Dr. Fodor was also a member of the Board of the IEEE Sweden Joint Communications, Information Theory and Vehicle Technology Chapter, from 2017 to 2020. He was a co-recipient of the IEEE Communications Society Stephen O. Rice Prize in 2018 and the Best Student Conference Paper Award from the IEEE Sweden VT/COM/IT Chapter in 2018. He is currently the Chair of the IEEE Communications Society Emerging Technology Initiative on Full Duplex Communications. He is currently serving as an Editor for IEEE TRANSACTIONS ON WIRELESS COMMUNICATIONS and IEEE WIRELESS COMMUNICATIONS.

Mikael Skoglund (Fellow, IEEE) received the Ph.D. degree from the Chalmers University of Technology, Sweden, in 1997. In 1997, he joined the Royal Institute of Technology (KTH), Stockholm, Sweden, where he was appointed to the Chair in communication theory in 2003. At KTH, he was the Head of the Division of Information Science and Engineering and also with the Department of Intelligent Systems. He has worked on problems in source-channel coding, coding and transmission for wireless communications, Shannon theory, information and control, and statistical signal processing. He has authored or coauthored more than 170 journal and 380 conference articles.

Dr. Skoglund has served on numerous technical program committees for IEEE sponsored conferences, he was a General Co-Chair of IEEE ITW 2019. He serves as a TPC Co-Chair for IEEE ISIT 2022. He was an Associate Editor of IEEE TRANSACTIONS ON COMMUNICATIONS from 2003 to 2008. From 2008 to 2012, he was on the Editorial Board of IEEE TRANSACTIONS ON INFORMATION THEORY.

Carlo Fischione (Senior Member, IEEE) received the Ph.D. degree in electrical and information engineering (3/3 years) and the Laurea degree *(summa cum laude)* in electronic engineering (5/5 years) from the University of L'Aquila, Italy, in April 2001 and May 2005, respectively. He has held research positions as a a Visiting Professor with the Massachusetts Institute of Technology, Cambridge, MA, USA, in 2015; also a Associate with Harvard University, Cambridge, in 2015; and also a Visiting Scholar and a Research Associate with the University of California at Berkeley, Berkeley, CA, USA, from 2004 to 2005 and from 2007 to 2008. Meanwhile, he also has offered his advice as a consultant to numerous technology companies such as ABB Corporate Research, Berkeley Wireless Sensor Network Lab, Ericsson Research, Synopsys, and United Technology Research Center. He is a Co-Founder and a Scientific Advisor of ELK. He is currently a Full Professor with the Electrical Engineering and Computer Science Department, Division of Network and Systems Engineering, KTH Royal Institute of Technology, Stockholm, Sweden. He is also the Director of the KTH-Ericsson Data Science Micro Degree Program and also a Chair of the IEEE Machine Learning for Communications Emerging Technologies Initiative. He is also an Honorary Professor with the Department of Mathematics, Information Engineering, and Computer Science, University of L'Aquila. He has coauthored more than 200 publications, including a book, book chapters, international journals and conferences, and international patents. His research interests include applied optimization, wireless, sensor networks, the Internet of Things, and machine learning.

Dr. Fischione received a number of awards, such as the "Ferdinando Filauro" Award from the University of L'Aquila in 2003, the "Higher Education" Award from Abruzzo Region Government, Italy, in 2004, the Best Paper Awards at the IEEE International Conference on Mobile Ad-hoc and Sensor System 05 and 09 (IEEE MASS 2005 and IEEE MASS 2009), the Junior Research Award from Swedish Research Council in 2007, the Best Paper Award of IEEE TRANSACTIONS ON INDUSTRIAL INFORMATICS in 2007, the Best Business Idea Awards from VentureCup East Sweden in 2010 and from Stockholm Innovation and Growth (STING) Life Science in Sweden in 2014, the "Silver Ear of Wheat" Award in history from the Municipality of Tornimparte, Italy, in 2012, the Best Paper Award of the IEEE Sweden VT-COM-IT Chapter in 2014, and the "IEEE Communication Society S. O. Rice" Award for the best IEEE TRANSACTIONS ON COMMUNICATIONS paper of 2018. He is an Ordinary Member of DASP (the Italian academy of history Deputazione Abruzzese di Storia Patria). He is an Editor of IEEE TRANSACTIONS ON COMMUNICATIONS and IEEE JOURNAL ON SELECTED AREAS ON COMMUNICATIONS—Series on Machine Learning for Communication and Networking. He has been serving as an Associate Editor for *Automatica* (IFAC) from 2014 to 2019.